Biogeosciences

Coupled eco-hydrology and biogeochemistry algorithms enable the simulation of water table depth effects on boreal peatland net CO$_2$ exchange

Mohammad Mezbahuddin[1,2]**, Robert F. Grant**[2]**, and Lawrence B. Flanagan**[3]

[1]Environmental Stewardship Branch, Alberta Agriculture and Forestry, Edmonton, AB, Canada
[2]Department of Renewable Resources, University of Alberta, Edmonton, AB, Canada
[3]Department of Biological Sciences, University of Lethbridge, AB, Canada

Correspondence to: Mohammad Mezbahuddin (symon.mezbahuddin@gov.ab.ca, mezbahud@ualberta.ca)

Abstract. Water table depth (WTD) effects on net ecosystem CO$_2$ exchange of boreal peatlands are largely mediated by hydrological effects on peat biogeochemistry and the eco-physiology of peatland vegetation. The lack of representation of these effects in carbon models currently limits our predictive capacity for changes in boreal peatland carbon deposits under potential future drier and warmer climates. We examined whether a process-level coupling of a prognostic WTD with (1) oxygen transport, which controls energy yields from microbial and root oxidation–reduction reactions, and (2) vascular and nonvascular plant water relations could explain mechanisms that control variations in net CO$_2$ exchange of a boreal fen under contrasting WTD conditions, i.e., shallow vs. deep WTD. Such coupling of eco-hydrology and biogeochemistry algorithms in a process-based ecosystem model, ecosys, was tested against net ecosystem CO$_2$ exchange measurements in a western Canadian boreal fen peatland over a period of drier-weather-driven gradual WTD drawdown. A May–October WTD drawdown of ~ 0.25 m from 2004 to 2009 hastened oxygen transport to microbial and root surfaces, enabling greater microbial and root energy yields and peat and litter decomposition, which raised modeled ecosystem respiration (R_e) by 0.26 µmol CO$_2$ m^{-2} s^{-1} per 0.1 m of WTD drawdown. It also augmented nutrient mineralization, and hence root nutrient availability and uptake, which resulted in improved leaf nutrient (nitrogen) status that facilitated carboxylation and raised modeled vascular gross primary productivity (GPP) and plant growth. The increase in modeled vascular GPP exceeded declines in modeled nonvascular (moss) GPP due to greater shading

from increased vascular plant growth and moss drying from near-surface peat desiccation, thereby causing a net increase in modeled growing season GPP by 0.39 µmol CO$_2$ m^{-2} s^{-1} per 0.1 m of WTD drawdown. Similar increases in GPP and R_e caused no significant WTD effects on modeled seasonal and interannual variations in net ecosystem productivity (NEP). These modeled trends were corroborated well by eddy covariance measured hourly net CO$_2$ fluxes (modeled vs. measured: $R^2 \sim 0.8$, slopes $\sim 1 \pm 0.1$, intercepts ~ 0.05 µmol m^{-2} s^{-1}), hourly measured automated chamber net CO$_2$ fluxes (modeled vs. measured: $R^2 \sim 0.7$, slopes $\sim 1 \pm 0.1$, intercepts ~ 0.4 µmol m^{-2} s^{-1}), and other biometric and laboratory measurements. Modeled drainage as an analog for WTD drawdown induced by climate-change-driven drying showed that this boreal peatland would switch from a large carbon sink (NEP ~ 160 g C m^{-2} yr^{-1}) to carbon neutrality (NEP ~ 10 g C m^{-2} yr^{-1}) should the water table deepen by a further ~ 0.5 m. This decline in projected NEP indicated that a further WTD drawdown at this fen would eventually lead to a decline in GPP due to water limitation. Therefore, representing the effects of interactions among hydrology, biogeochemistry and plant physiological ecology on ecosystem carbon, water, and nutrient cycling in global carbon models would improve our predictive capacity for changes in boreal peatland carbon sequestration under changing climates.

1 Introduction

Northern boreal peatlands have been accumulating carbon (C) at a rate of about 20–$30 \, \mathrm{g \, m^{-2} \, yr^{-1}}$ over several thousand years (Gorham, 1991; Turunen et al., 2002). Drier and warmer future climates can affect the resilience of long-term boreal peatland C stocks by lowering the water table (WT) that can halt or even reverse the C accumulation in boreal peatlands (Limpens et al., 2008; Dise, 2009; Frolking et al., 2011). To maintain and protect the C sequestration potentials of boreal peatlands, we need an improved predictive capacity of how these C stocks would behave under future drier and warmer climates. However, boreal peatland C processes are currently underrepresented in global C models largely due to an inadequate simulation of hydrologic feedbacks to C cycles (St-Hilaire et al., 2010; Sulman et al., 2012). This can be overcome by integrating interactions between eco-hydrology of peatland vegetation and peat biogeochemistry into finer-resolution process models that can eventually be scaled up into larger spatial- and temporal-scale C models (Waddington et al., 2015).

The hydrologic feedbacks to boreal peatland C processes are largely mediated by water table depth (WTD) variation and its effects on peat-microbe-plant-atmosphere exchanges of C, energy, water and nutrients (Grant et al., 2012). WTD drawdown can affect net ecosystem productivity (NEP) of boreal peatlands through its effects on ecosystem respiration (R_e) and gross primary productivity (GPP). A receding WT can cause peat pore drainage that enhances microbial O_2 availability, energy yields, growth and decomposition and hence increases R_e (Sulman et al., 2009, 2010; Cai et al., 2010; Flanagan and Syed, 2011; Peichl et al., 2014). The rate of increase in R_e due to the WTD drawdown may vary with peat moisture retention and quality of peat-forming substrates (Preston et al., 2012). For instance, peats with low moisture retention capacities exhibit more rapid pore drainage than those with high moisture retention, thus causing more increase in R_e for similar WTD drawdowns (Parmentier et al., 2009; Sulman et al., 2009, 2010; Cai et al., 2010). Peats formed from *Sphagnum* mosses degrade at rates slower than those formed from remains of vascular plants (Moore and Basiliko, 2006). So for similar WTD drawdowns, moss peats would experience less increase in microbial decomposition and hence R_e than would sedge, reed, or woody peats (Updegraff et al., 1995). Continued WTD drawdown can also cause near-surface peat desiccation from inadequate recharge through capillary rise from deeper WT. The desiccation of near-surface shallow peat layers can cause a reduction in microbial decomposition that can partially or fully offset the increased decomposition in the deeper peat layers, thereby yielding indistinct net effects of WTD drawdown on R_e (Dimitrov et al., 2010a).

The interactions between WTD and GPP vary across peatlands depending upon peat-forming vegetation. For instance, increased aeration due to WTD drawdown enhances root O_2 availability and growth in vascular plants (Lieffers and Rothwell, 1987; Murphy et al., 2009). Enhanced root growth is also associated with greater root nutrient availability and uptake from more rapid mineralization facilitated by greater microbial energy yields, growth and decomposition under a deeper WT (Choi et al., 2007). Greater root nutrient uptake increases the rate of vascular CO_2 fixation and hence GPP (Sulman et al., 2009, 2010; Cai et al., 2010; Flanagan and Syed, 2011; Peichl et al., 2014). WTD drawdown, however, does not affect the nonvascular (e.g., moss) GPP in the same way it does the vascular GPP (Lafleur et al., 2005). Nonvascular plants mostly depend upon the water available for uptake in the near-surface shallow peat layers (Dimitrov et al., 2011). These layers can drain quickly with receding WT and thus have to depend on moisture supply through capillary rise from deeper WT (Dimitrov et al., 2011; Peichl et al., 2014). If recharge through the capillary rise is not adequate, near-surface peat desiccation occurs which slows moss water uptake, causes eventual drying of mosses and reduces moss GPP (Lafleur et al., 2005; Riutta 2008; Sonnentag et al., 2010; Sulman et al., 2010; Dimitrov et al., 2011; Kuiper et al., 2014; Peichl et al., 2014). Near-surface peat desiccation also suppresses vascular root water uptake from the desiccated layers (Lafleur et al., 2005; Dimitrov et al., 2011). But enhanced root growth and elongation facilitated by improved O_2 status in the newly aerated deeper peat layers under a deeper WT enables vascular roots to take up water from wetter deeper layers (Dimitrov et al., 2011). If deeper root water uptake offsets the reduction in water uptake from desiccated near-surface layers, vascular transpiration (T), canopy stomatal conductance (g_c), and hence GPP are sustained under a deeper WT (Dimitrov et al., 2011). But if the WT falls below a certain threshold level under which deeper root water uptake can no longer sustain vascular T, g_c and hence vascular GPP declines (Lafleur et al., 2005; Wu et al., 2010).

WTD variation can thus affect boreal peatland NEP through its effects on peat moisture and aeration and consequent root and microbial oxidation–reduction reactions and energy yields. To predict how boreal peatlands would behave under future drier and warmer climates, a peatland C model thus needs to simulate WTD dynamics that determine the boundary between aerobic and anaerobic zones and control peat biogeochemistry. However, most of the current process-based peatland C models either do not simulate a continuous anaerobic zone below a prognostic WT (e.g., Baker et al., 2008; Schaefer et al., 2008; Tian et al., 2010) or do not simulate peat saturation since any water in excess of field capacity is drained in those models (e.g., Gerten et al., 2004; Krinner et al., 2005; Weng and Luo, 2008). Moreover, instead of explicitly simulating the above-described hydrological and biological interactions between peat aeration and biogeochemistry, most of those models use scalar functions of soil moisture contents to inhibit R_e and GPP under low or high moisture conditions (e.g., Frolking et al., 2002; Zhang et al., 2002; Bond-Lamberty et al., 2007; St-Hilaire et al.,

2010; Sulman et al., 2012). Consequently, those peatland C models could not simulate declines in GPP and R_e due to shallow WT while simulating WTD effects on CO_2 exchange of peatlands across the northern US and Canada (Sulman et al., 2012). Furthermore, the approach of using scalar functions to simulate moisture limitations to GPP and R_e requires site-specific parameterization of model algorithms, which reduces the scalability of those peatland C models.

2 Objective and rationale

In this study, we tested a process-based ecosystem model, ecosys, against eddy covariance (EC) net CO_2 fluxes measured over a drying period from 2004 to 2009 in a western Canadian boreal fen peatland in Alberta, Canada (termed as WPL hereafter) (Syed et al., 2006; Flanagan and Syed, 2011). The objective was to test whether the coupling of a dynamic WTD that arises from vertical and lateral water fluxes as a function of a soil moisture retention scheme with (1) oxygen transport, (2) microbial and root oxidation–reduction reactions and energy yields, and (3) root, microbial and plant growth and uptake within a soil–plant–microbe–atmosphere water, C and nutrient (nitrogen, phosphorus) scheme in an ecosystem process model could explain underlying processes that govern hydrological effects on net CO_2 exchange of a northern boreal fen under contrasting WTD conditions (e.g., shallower vs. deeper WTD). This study would reconcile our knowledge on the feedback mechanisms among hydrology, ecophysiology and biogeochemistry of peatlands, which is predominantly based upon inferences drawn from EC gap-filled values that include empirically modeled estimates. It would also provide us with a better insight into – and an improved predictive capacity of – how carbon deposits in northern boreal peatlands would behave under changing climates. Rigorous site-scale testing of coupled eco-hydrology and biogeochemistry algorithms in ecosystem process models such as ecosys would also provide us with important insights on how to improve large-scale representation of these processes into next-generation land surface models.

2.1 Hypotheses

In an EC study, Flanagan and Syed (2011) found no net effect of a drier-weather-driven WTD drawdown on NEP at the WPL over 2004–2009. From the regressions of EC-derived GPP and R_e on site-measured WTD, they inferred that the absence of a net WTD effect on NEP was caused by similar increases in GPP and R_e with WTD drawdown. We hypothesized that coupled eco-hydrology and biogeochemistry algorithms in ecosys would be able to simulate and explain underlying mechanisms of these effects of WTD drawdown on GPP and R_e and hence NEP at the WPL. We tested the following four central hypotheses:

1. WTD drawdown would increase R_e of the northern fen at the WPL. This effect of WTD drawdown on R_e would be modeled by the simulation of peat pore drainage and improved peat aeration that would increase the energy yields from aerobic microbial decomposition and hence would increase R_e.

2. WTD drawdown would increase GPP of the northern fen at the WPL. This effect of WTD drawdown on GPP would be modeled by simulating enhanced microbial activity due to WTD drawdown that would cause more rapid nutrient mineralization and greater root nutrient availability and uptake, greater leaf nutrient concentrations and hence increased GPP.

3. An increase in R_e with WTD drawdown (hypothesis 1) would cease should WTD fall below a threshold depth. This threshold WTD effect on R_e would be modeled by simulating inadequate recharge of the near-surface peat layers through capillary rise from the deeper WTD below the threshold level that would cause desiccation of those layers. Drying of near-surface peat layers and the surface residue would reduce near-surface and surface peat respiration that would partially offset the increase in deeper peat respiration due to aeration.

4. The net effect of threshold WTD on GPP would be driven by the balance between how WTD would affect vascular vs. nonvascular GPP. This threshold WTD effect on GPP would be modeled by simulating vascular vs. nonvascular water relations under deeper WTD below the threshold level. Near-surface peat desiccation in hypothesis 3 would reduce peat water potential and hydraulic conductivity and hence vascular and nonvascular water uptake from desiccated near-surface layers. Since nonvascular mosses depend mainly on near-surface peat layers for moisture supply, reduction in moss water uptake would cause a reduction in moss water potential and hence moss GPP. By contrast, the suppression of vascular root water uptake from desiccated near-surface layers under a deeper WT would be offset by increased deeper root water uptake from newly aerated deeper peat layers with higher water potentials that would sustain vascular canopy water potential (ψ_c), g_c and GPP.

3 Methods

3.1 Model development

Ecosys is a process-based ecosystem model which simulated 3-D water, energy, carbon and nutrient (nitrogen, phosphorus) cycles in different peatlands (Dimitrov et al., 2011; Grant et al., 2012; Sulman et al., 2012; Mezbahuddin et al.,
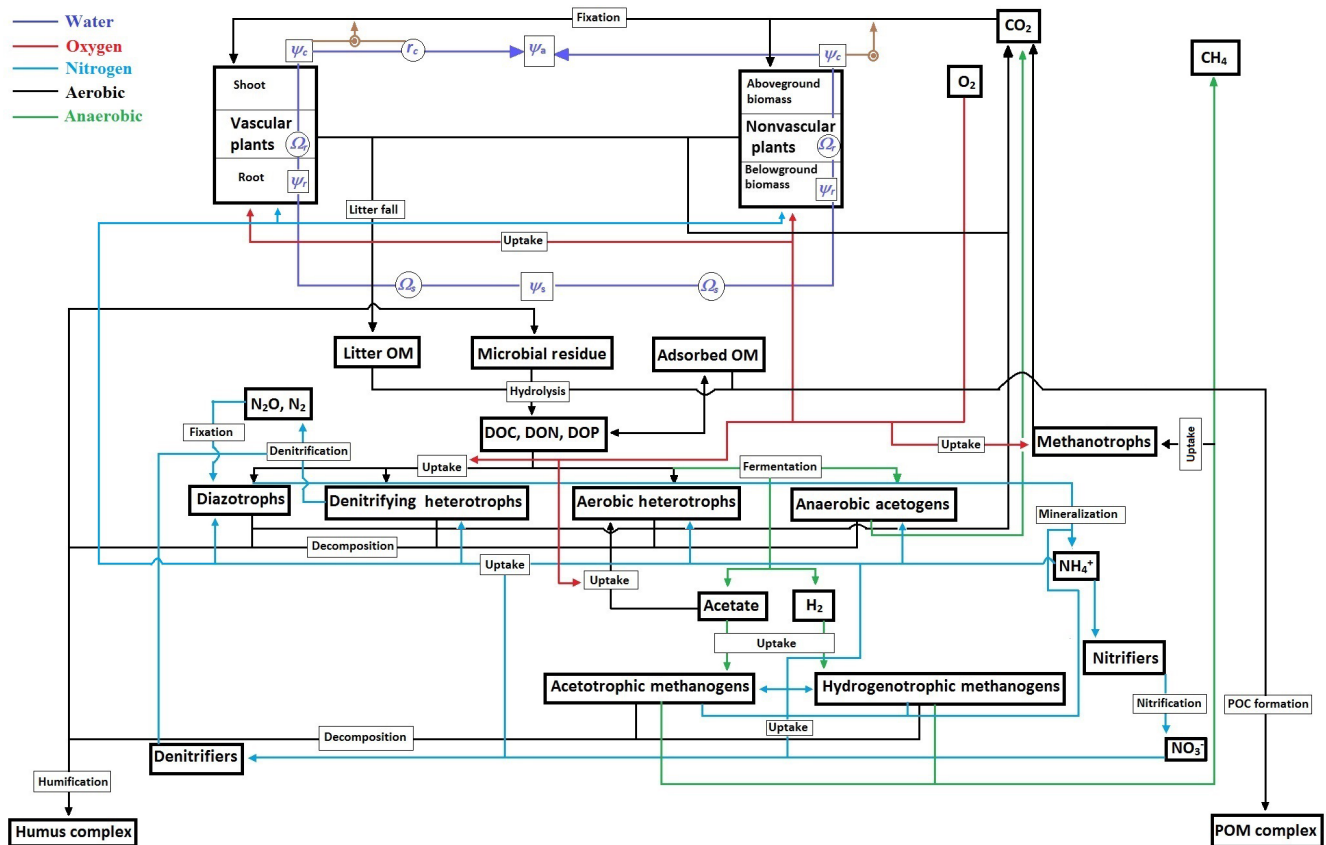
Figure 1. Schematic diagram of ecosys algorithms representing coupled key eco-physiological and biogeochemical (aerobic and anaerobic) processes and plant water relations of a typical boreal fen peatland ecosystem that are affected by WTD fluctuation. Ψ_a, Ψ_c and Ψ_s: atmospheric, canopy and soil water potentials; Ψ_r: vascular root or nonvascular belowground water potential; r_c: canopy stomatal resistance ($1/g_c$); Ω_s: soil hydraulic resistance; Ω_r: hydraulic resistance to water flow through plants; OM: organic matter; DOC, DON, DOP: dissolved organic carbon, nitrogen and phosphorus; POC: particulate organic C; and POM: particulate organic matter.

2014, 2015, 2016). Ecosys algorithms that govern the modeled effects of WTD variations on peatland net CO_2 exchange are described below. These algorithms in ecosys are derived from published independent basic research which describes eco-hydrological and biogeochemical mechanisms that govern the carbon, nutrient (N, P), water and energy balance of a typical boreal peatland ecosystem (Fig. 1). Ecosys algorithms which are related to our hypotheses are depicted as a flowchart (Fig. 1) and cited as equations within the text. These equations are also listed in appendices A to D in the Supplement. These site-independent basic ecosystem process algorithms in ecosys are thus not parameterized for each peatland site. Instead the coupled algorithms are fed with peatland-specific measurable soil, weather, vegetation and management inputs to simulate the C, nutrient (N, P), water and energy balance of a particular peatland ecosystem.

3.1.1 Water table depth

The WTD in ecosys is calculated at the end of each time step as the depth to the top of the saturated zone, below which air-

filled porosity is 0 (Eq. SD32). It is the depth at which lateral water flux is in equilibrium with the difference between vertical influxes (precipitation) and effluxes (evapotranspiration). Lateral water transfer between modeled grid cells in ecosys and the adjacent ecosystem occurs to and from a set external WTD (WTD$_x$) over a set distance (L_t) (Fig. 2). The WTD$_x$ represents average watershed WTD with reference to average hummock surface. The WTD in ecosys is thus not prescribed but rather controls, and is controlled by, lateral and vertical surface and subsurface water fluxes (Eqs. SD1–SD31). More detail about how peatland WTD, vertical and lateral soil water flow and soil moisture retention are modeled in ecosys can be found in Dimitrov et al. (2010b) and Mezbahuddin et al. (2015, 2016).

3.1.2 Heterotrophic respiration and WTD

WTD fluctuation in ecosys determines the boundary between and the extent of aerobic vs. anaerobic soil zones. So, WTD fluctuation affects ecosys's algorithms of organic oxidation–reduction transformations and microbial energy
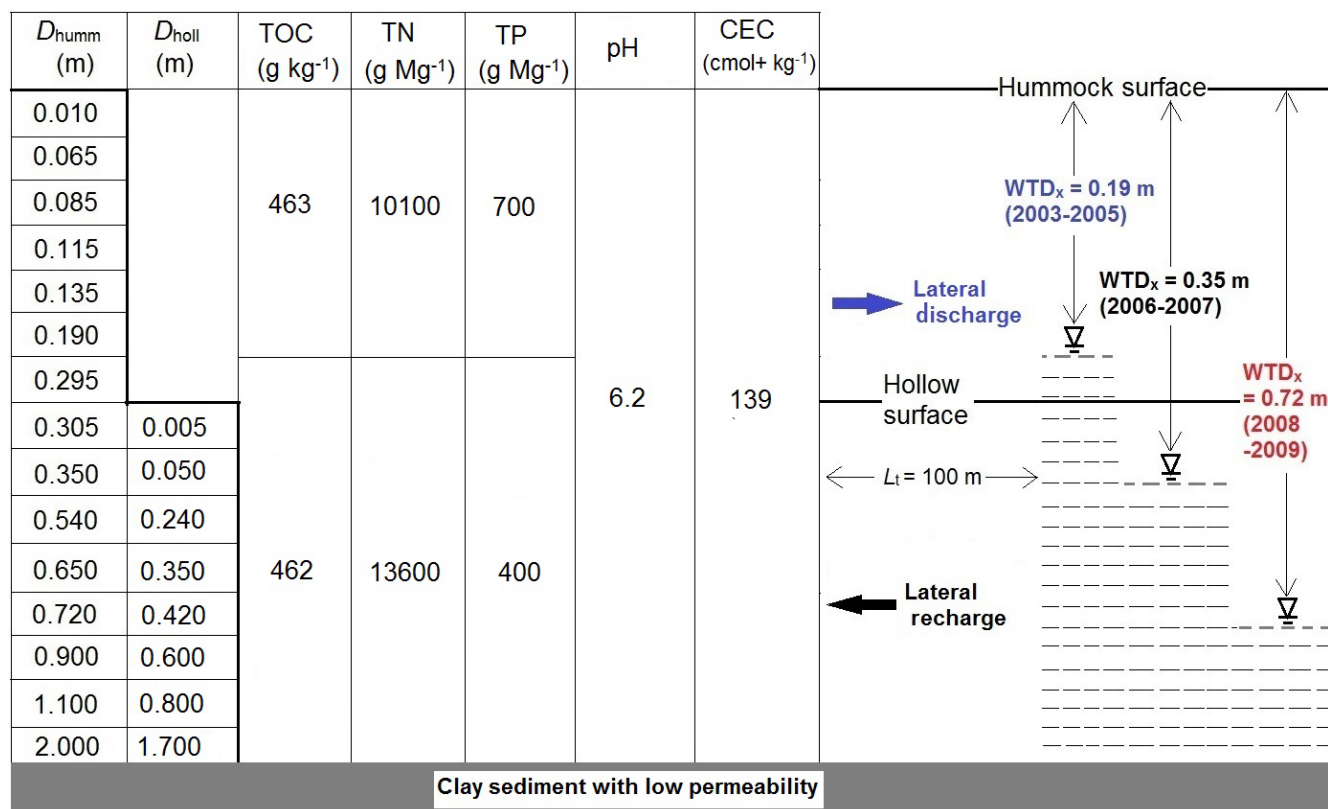
D_{humm} (m)	D_{holl} (m)	TOC (g kg^{-1})	TN (g Mg^{-1})	TP (g Mg^{-1})	pH	CEC (cmol+ kg^{-1})
0.010						
0.065						
0.085		463	10100	700		
0.115						
0.135						
0.190						
0.295						
0.305	0.005				6.2	139
0.350	0.050					
0.540	0.240					
0.650	0.350	462	13600	400		
0.720	0.420					
0.900	0.600					
1.100	0.800					
2.000	1.700					

Figure 2. Layout for ecosys model run to represent biological, chemical and hydrological characteristics of a western Canadian fen peatland. Figure is not drawn to scale. D_{humm}: depth to the bottom of a layer from the hummock surface; D_{holl}: depth to the bottom of a layer from the hollow surface; TOC: total organic C (Flanagan and Syed, 2011); TN: total nitrogen (Flanagan and Syed, 2011); TP: total phosphorus (Flanagan and Syed, 2011); CEC: cation exchange capacity (Rippy and Nelson, 2007) – the value for pH was obtained from Syed et al. (2006); WTD$_x$: external reference water table depth representing average water table depth of the adjacent ecosystem; L_t: distance from modeled grid cells to the adjacent watershed over which lateral discharge/recharge occurs.

yields, which drive microbial growth and substrate decomposition and uptake (Fig. 1) (Eqs. SA1–SA30). Organic transformations in ecosys occur in a residue layer and in each of the user-defined soil layers within five organic-matter–microbe complexes, i.e., coarse woody litter, fine nonwoody litter, animal manure, particulate organic C and humus (Fig. 1). Each of the complexes has three decomposition substrates, i.e., solid organic C, sorbed organic C and microbial residue C; the decomposition agent, i.e., microbial biomass; and the decomposition product, i.e., dissolved organic C (DOC) (Fig. 1). The rates of the decomposition and resulting DOC production in each of the complexes are a first-order function of the fraction of substrate colonized by active biomasses (M) of diverse microbial functional types (MFTs). The MFTs in ecosys are obligate aerobes (bacteria and fungi), facultative anaerobes (denitrifiers), obligate anaerobes (fermenters), heterotrophic (acetotrophic) and autotrophic (hydrogenotrophic) methanogens, and aerobic and anaerobic heterotrophic diazotrophs (nonsymbiotic N$_2$ fixers) (Fig. 1) (Eqs. SA1–SA2, SA4). Biomass (M) growth of each of the MFTs (Eq. SA25a) is calculated from its DOC

uptake (Fig. 1) (Eq. SA21). The rate of M growth is driven by energy yield from growth respiration (R_g) (Eq. SA20) that is calculated by subtracting maintenance respiration (R_m) (Eq. SA18) from heterotrophic respiration (R_h) (Eq. SA11). The values of R_h are driven by oxidation of DOC (Eq. SA13). DOC oxidation may be limited by microbial O$_2$ reduction (Eq. SA14) driven by microbial O$_2$ demand (Eq. SA16) and constrained by O$_2$ diffusion calculated from aqueous O$_2$ concentrations in soil ([O$_{2s}$]) (Eq. SA17). Values of [O$_{2s}$] are maintained by convective–dispersive transport of O$_2$ from the atmosphere to gaseous and aqueous phases of the soil surface layer (Eq. SD41), by convective–dispersive transport of O$_2$ through gaseous and aqueous phases in adjacent soil layers (Eqs. SD42, SD44), and by the dissolution of O$_2$ from gaseous to aqueous phases within each soil layer (Eq. SD39).

Shallow WTD in ecosys can cause lower air-filled porosity (θ_g) in the wetter peat layers above the WT. Lower θ_g reduces O$_2$ diffusivity in the gaseous phase (D_g) (Eq. SD44) and gaseous O$_2$ transport (Eqs. SD41–SD42) in these layers. Peat layers below the WT have zero θ_g that prevents gaseous O$_2$ transport in these layers. So, under a shallow

WT, $[O_{2s}]$ relies more on O_2 transport through the slower aqueous phase (Eq. SD42), which causes a decline in $[O_{2s}]$. A decline in $[O_{2s}]$ slows O_2 uptake (Eq. SA17) and hence R_h (Eq. SA14), R_g (Eq. SA20) and the growth of M (Eq. SA25). Lower M slows decomposition of organic C (Eqs. SA1–SA2) and production of DOC, which further slows R_h (Eq. SA13), R_g and the growth of M (Fig. 1). Although some MFTs can sustain DOC oxidation by reducing alternative electron acceptors (e.g., methanogens reducing acetate or CO_2 to CH_4 and denitrifiers reducing NO_x to N_2O or N_2), lower energy yields from these reactions reduce R_g (Eq. SA21) and hence M growth, organic C decomposition and subsequent DOC production (Fig. 1). Slower decomposition of organic C under low $[O_{2s}]$ also causes slower decomposition of organic nitrogen (N) and phosphorus (P) (Eq. SA7) and the production of dissolved organic nitrogen (DON) and phosphorus (DOP), which causes slower uptake of microbial N and P (Eq. SA22) and growth of M (Eq. SA29) (Fig. 1). Slower M growth causes slower mineralization (Eq. SA26) and hence lowers aqueous concentrations of NH_4^+, NO_3^- and $H_2PO_4^-$ (Fig. 1).

WTD drawdown can increase θ_g that results in greater D_g (Eq. SD44) and more rapid gaseous O_2 transport. A consequent rise in $[O_{2s}]$ increases O_2 uptake (Eq. SA17) and R_h (Eq. SA14), R_g (Eq. SA20) and the growth of M (Eq. SA25). Larger M hastens the decomposition of organic C (Eqs. SA1–SA2) and the production of DOC which further hastens R_h (Eq. SA13), R_g and the growth of M. More rapid decomposition of organic C under adequate $[O_{2s}]$ in this period also causes more rapid decomposition of organic N and P (Eq. SA7) and production of DON and DOP, which increases the uptake of microbial N and P (Eq. SA22) and the growth of M (Eq. SA29) (Fig. 1). Rapid M growth causes rapid mineralization (Eq. SA26) and hence greater aqueous concentrations of NH_4^+, NO_3^- and $H_2PO_4^-$ (Fig. 1).

When WTD recedes below a certain threshold level, capillary rise from the WT can no longer support adequate recharge of the near-surface peat layers and the surface litter (Eqs. SD9, SD12). It causes desiccation of the residue and the near-surface peat layers, thereby causing a reduction in water potential (ψ_s) and an increase in aqueous microbial concentrations ($[M]$) in each of these layers (Eq. SA15). Increased $[M]$ caused by the peat desiccation reduces microbial access to the substrate for decomposition in each of the desiccated layers and reduces R_h (Eq. SA13). The reduction in R_h is calculated in ecosys from competitive inhibition of microbial exoenzymes with increasing concentrations (Eq. SA4) (Lizama and Suzuki, 1991).

3.1.3 WTD effects on vascular gross primary productivity

Ecosys simulates effects of WTD variation on vascular GPP from WTD variation effects on root O_2 and nutrient availability and root growth and uptake. Root O_2 and nutrient up-

take in ecosys are coupled with a hydraulically driven soil–plant–atmosphere water scheme. Root growth in each vascular plant population in ecosys is calculated from its assimilation of the nonstructural C product of CO_2 fixation (σ_C) (Eq. SC20). Assimilation is driven by R_g (Eq. SC17) remaining after subtracting R_m (Eq. SC16) from autotrophic respiration (R_a) (Eq. SC13) driven by oxidation of σ_C (Eq. SC14). Oxidation in roots may be limited by root O_2 reduction (Eq. SC14b), which is driven by root O_2 demand to sustain C oxidation and nutrient uptake (Eq. SC14e), and constrained by O_2 uptake controlled by concentrations of aqueous O_2 in the soil ($[O_{2s}]$) and roots ($[O_{2r}]$) (Eq. SC14d). Values of $[O_{2s}]$ and $[O_{2r}]$ are maintained by convective–dispersive transport of O_2 through soil gaseous and aqueous phases and root gaseous phase (aerenchyma), respectively, and by dissolution of O_2 from soil and root gaseous to aqueous phases (Eqs. SD39–SD45). O_2 transport through root aerenchyma depends on species-specific values used for root air-filled porosity (θ_{pr}) (Eq. SD45). Shallow WTD and resultant high peat moisture content in ecosys can cause low θ_g that reduces soil O_2 transport, forcing root O_2 uptake to rely more on $[O_{2r}]$ and hence on root O_2 transport determined by θ_{pr}. If this transport is inadequate, a decline in $[O_{2r}]$ slows root O_2 uptake (Eq. SC14c–d) and hence R_a (Eq. SC14b), R_g (Eq. SC17) and root growth (Eq. SC20b) and root N and P uptake (Eqs. SC23b, d, f) (Fig. 1). Root N and P uptake under a shallow WT is further slowed by reductions in aqueous concentrations of NH_4^+, NO_3^- and $H_2PO_4^-$ (Eqs. SC23a, c, e) from slower mineralization of organic N and P (Fig. 1). Slower root N and P uptake reduces concentrations of nonstructural N and P products of root uptake (σ_N and σ_P) with respect to that of σ_C in leaves (Eq. SC11), thereby slowing CO_2 fixation (Eq. SC6) and GPP.

WTD drawdown facilitates rapid D_g which allows root O_2 demand to be almost entirely met from $[O_{2s}]$ (Eqs. SC14c–d) and so enables more rapid root growth and N and P uptake (Eqs. SC23b, d, f). Increased root growth and nutrient uptake is further stimulated by increased aqueous concentrations of NH_4^+, NO_3^- and $H_2PO_4^-$ (Eqs. SC23a, c, e) from more rapid mineralization of organic N and P during deeper WT (Fig. 1). Greater root N and P uptake increases concentrations of σ_N and σ_P with respect to σ_C in leaves (Eq. SC11), thereby facilitating rapid CO_2 fixation (Eq. SC6) and GPP. when the WT falls below a certain threshold, inadequate capillary rise (Eqs. SA9, SA12) from deeper WT causes near-surface peat desiccation that reduces ψ_s and raises soil hydraulic resistance (Ω_s) (Eq. SB9), thereby forcing lower root water uptake (U_w) from desiccated layers (Fig. 1) (Eq. SB6). However, deeper rooting facilitated by increased $[O_{2s}]$ under a deeper WT can sustain U_w (Eq. SB6) from wetter deeper peat layers with higher ψ_s and lower Ω_s (Eq. SB9). If U_w from the deeper wetter layers cannot offset the suppression in U_w from desiccated near-surface layers, the resultant net decrease in U_w causes a reduction in root (ψ_r), canopy and turgor potentials (ψ_t) (Eq. SB4) and hence g_c (Eq. SB2b) in ecosys when

equilibrating U_w with transpiration (T) (Eq. SB14). Lower g_c reduces CO_2 diffusion into the leaves, thereby reducing CO_2 fixation (Eq. SC6) and GPP (Eq. SC1) (Fig. 1).

3.1.4 WTD effects on nonvascular gross primary productivity

Ecosys simulates nonvascular plants (e.g., mosses) as tiny plants with no stomatal regulations that grow on modeled hummock and hollow grid cells (Dimitrov et al., 2011). Model input for moss population is usually larger and hence intraspecific competition for lights and nutrients is greater so that individual moss plant and moss belowground growth (i.e., root like structures for water and nutrient uptake) are smaller (Eq. SC21b). Shallower belowground growth of simulated mosses in ecosys means that the water uptake of mosses is mostly confined to the near-surface peat layers. when the WT deepens past a threshold level, inadequate capillary rise (Eqs. SD9, SD12) causes near-surface peat desiccation, thereby reducing ψ_s and increasing Ω_s (Eq. SB9) of those layers (Fig. 1). Reduced ψ_s along with increased Ω_s causes a reduction in moss ψ_c while equilibrating moss evaporation with moss U_w (Eq. SB6). Reduced moss ψ_c causes a reduction in moss carboxylation rate (Eqs. SC3, SC6a) and moss GPP (Fig. 1) (Eq. SC1).

3.2 Modeling experiment

3.2.1 Study site

Eco-hydrology and biogeochemistry algorithms in ecosys were tested in this study against measurements of WTD and ecosystem net CO_2 fluxes at a flux station of the FLUXNET-Canada Research Network established at the WPL (latitude: 54.95° N; longitude: 112.47° W). The study site is a moderately nutrient-rich treed fen peatland within the central mixed-wood subregion of boreal alberta, Canada. Peat depth around the flux station was about 2 m. This peatland is dominated by stunted trees of black spruce (*Picea mariana*) and tamarack (*Larix laricina*) with an average canopy height of 3 m. A high abundance of a shrub species *Betula pumila* (dwarf birch) and the presence of a wide range of mosses, e.g., *Sphagnum* spp., feather moss and brown moss characterize the understory vegetation of WPL. The topographic, climatic, edaphic and vegetative characteristics of this site were described in more details by Syed et al. (2006).

3.2.2 Field data sets

Ecosys model inputs of half-hourly weather variables, i.e., incoming shortwave and longwave radiation, air temperature (T_a), wind speed, precipitation and relative humidity during 2003–2009, were measured by Syed et al. (2006) and Flanagan and Syed (2011) at the micrometeorological station installed at the WPL. To test the adequacy of WTD simulation in ecosys, modeled outputs of hourly WTD were tested

against WTD measured at the WPL with respect to average hummock surface by Flanagan and Syed (2011) (Mezbahuddin et al., 2016). To examine how well ecosys simulated the net ecosystem CO_2 exchange at the WPL, we tested hourly modeled net ecosystem CO_2 fluxes against hourly averaged measurements (average of two half-hourly measurements) collected by Syed et al. (2006) and Flanagan and Syed (2011) by using an EC micrometeorological approach. Each of these EC-measured net CO_2 fluxes consisted of an eddy flux and a storage flux (Syed et al., 2006). Erroneous flux measurements due to stable air conditions were screened out with the use of a minimum friction velocity (u^*) threshold of $0.15\,\mathrm{m\,s^{-1}}$ (Syed et al., 2006). The net CO_2 fluxes that survived the quality control were used to derive half-hourly R_e (nighttime net CO_2 fluxes) and GPP (daytime net CO_2 fluxes – R_e) (Barr et al., 2004; Syed et al., 2006). To derive daily, seasonal and annual estimates of GPP and R_e, the data gaps resulting from the quality control were filled based on empirical relationships between soil temperature at a shallow depth (0.05 m) and measured half-hourly R_e and between incoming shortwave radiation and measured half-hourly GPP using 15-day moving windows. The gap-filled R_e and GPP were then summed up for each half hour to fill NEP data gaps to derive daily, seasonal and annual estimates of EC gap-filled NEP (Barr et al., 2004; Syed et al., 2006).

Soil CO_2 fluxes measured by automated chambers can provide a valuable supplement to EC CO_2 fluxes in testing modeled respiration by providing more continuous measurements than EC. So, we tested our modeled outputs against half-hourly automated chamber measurements by Cai et al. (2010) at the WPL. These CO_2 flux measurements were carried out during ice-free periods (May–October) of 2005 and 2006 over both hummocks and hollows by using a total of nine non-steady-state automatic transparent chambers (Cai et al., 2010). Along with soil respiration these chamber CO_2 fluxes included fixation and autotrophic respiration from dwarf shrubs, herbs and mosses (Cai et al., 2010).

Modeled WTD effects on peatland biogeochemistry and hence on peatland nutrient and carbon cycling were also corroborated against leaf nitrogen concentrations, foliar N-to-P ratios, N mineralization, and rooting depths biometrically measured at either our site or at sites that had similar peat substrates, hydrology and/or plant functional types. Needles of black spruce and tamarack and leaves of dwarf birch were sampled over our study site during midsummer of 2004 for foliar nutrient content analyses (Syed et al., 2006). Leaf nitrogen contents were analyzed on N_2 gas that was generated from the reduction of dried leaf tissues in an elemental analyzer and quantified using a gas isotope ratio mass spectrometer (Syed et al., 2006). Leaf phosphorus contents were analyzed on black spruce and tamarack needle leaf tissues that were dry-ashed and then digested using a dilute HNO_3 and HCl mixture and then quantified using an inductively coupled plasma (ICP) spectroscopic analysis technique (Syed et al., 2006).

3.2.3 Model run

An ecosys model run to simulate WTD effects on net CO_2 exchange of WPL had a hummock and a hollow grid cell that exchanged water, heat, carbon and nutrients (N, P) between them and with surrounding vertical and lateral boundaries (Fig. 2). The hollow grid cell had a near-surface peat layer that was 0.3 m thinner than the hummock cell representing a hummock–hollow surface difference of 0.3 m observed in the field (Long, 2008) (Fig. 2). Any depth with respect to the modeled hollow surface would thus be 0.3 m shallower than the depth with respect to the modeled hummock surface.

Peat organic and chemical properties at different depths of the WPL were represented in ecosys by inputs from measurements either at the site (e.g., Syed et al., 2006; Flanagan and Syed, 2011) or at similar nearby sites (e.g., Rippy and Nelson, 2007) (Fig. 2). Ecosys was run for a spin-up period of 1961–2002 under repeating 7-year sequences of hourly weather data (shortwave and longwave radiation, air temperature, wind speed, humidity and precipitation) recorded at the site from 2003 to 2009. There was a drying trend observed from 2003 to 2009 due to diminishing precipitation that caused WTD drawdown in the watershed in which WPL is located, which lowered the WT of this fen peatland (Flanagan and Syed, 2011). To accommodate the gradual drying effects of catchment hydrology on modeled fen peatland WTD, we set the WTD_x at different levels based on the annual wetness of weather, e.g., shallow, intermediate, and deep ($WTD_x = 0.19$, 0.35 and 0.72 m below the hummock surface or 0.11 m above and 0.05 and 0.42 m below the hollow surface) (Fig. 2). There was no exchange of water through the lower model boundary to represent the presence of nearly impermeable clay sediment underlying the peat (Syed et al., 2006) (Fig. 2). Variations in peat surface with WTD variations, which are an important hydrologic self-regulation of boreal peatlands (Dise, 2009), were not represented in this version of ecosys.

At the start of the spin-up run, the hummock grid cell was seeded with an evergreen needle leaf and a deciduous needle leaf overstory plant functional type (PFT) to represent the black spruce and tamarack trees at the WPL. The hollow grid cell was seeded with only the deciduous needle leaf overstory PFT since the black spruce trees at the WPL only grew on the raised areas. Each of the modeled hummock and the hollow was also seeded with a deciduous broadleaved vascular (to represent dwarf birch) and a nonvascular (to represent mosses) understory PFTs. The planting densities were such that the population densities of the black spruce, tamarack, dwarf birch and moss PFTs were 0.16, 0.14, 0.3, and 500 m^{-2}, respectively, at the end of the spin-up run so as to best represent field vegetation (Syed et al., 2006; Mezbahuddin et al., 2016). To include wetland adaptation, we used a root porosity (θ_{pr}) value of 0.1 for the two overstory PFTs and a higher θ_{pr} value of 0.3 for the understory vascular PFT to represent better wetland adaptation in the understory than the overstory PFTs. These θ_{pr} values were used in calculating root O_2 transport through aerenchyma (Eq. SD45) and did not change with waterlogging throughout the model run. These θ_{pr} values were representatives of root porosities measured for various northern boreal peatland plant species (Cronk and Fennessy, 2001). Nonsymbiotic N_2 fixation through the association of cyanobacteria and mosses are also reported for Canadian boreal forests (Markham, 2009). This was represented in ecosys as N_2 fixation by nonsymbiotic heterotrophic diazotrophs (Eq. SA27) in the moss canopy. Further details about ecosys model setup to represent the hydrological, physical and ecological characteristics of WPL can be found in Mezbahuddin et al. (2016).

When the modeled ecosystem attained stable values of net ecosystem CO_2 exchange at the end of the spin-up run, we continued the spin-up run into a simulation run from 2003 to 2009 by using a real-time weather sequence. We tested our outputs from 2004 to 2009 of the simulation run against the available site measurements of WTD, net EC CO_2 fluxes and net chamber CO_2 fluxes over those years.

3.2.4 Model validation

To examine the adequacy of modeling WTD effects on canopy, root and soil CO_2 fluxes, which were summed for net ecosystem CO_2 exchange at the WPL, we spatially averaged hourly net CO_2 fluxes modeled over the hummock and the hollow to represent a 50 : 50 hummock–hollow ratio; they were regressed against hourly EC-measured net ecosystem CO_2 fluxes for each year from 2004 to 2009 with varying WTD. Each of these hourly EC-measured net ecosystem CO_2 fluxes used in these regressions is an average of two half-hourly net CO_2 fluxes measured at a friction velocity (u^*) greater than 0.15 m s^{-1} that survived quality control procedure (Sect. 3.2.2). Model performance was evaluated from regression intercepts ($a \rightarrow 0$), slopes ($b \rightarrow 1$), coefficients of determination ($R^2 \rightarrow 1$), and root means squares for errors (RMSE $\rightarrow 0$) for each study year to test whether there was any systematic divergence between the modeled and EC-measured CO_2 fluxes.

Similar regressions were performed between modeled and automated chamber-measured net CO_2 fluxes for ice-free periods (May–October) of 2005 and 2006 to further test the robustness of modeled soil respiration under contrasting WTD conditions. Each of the half-hourly measured chamber net CO_2 fluxes included soil respiration and fixation and autotrophic respiration from understory vegetation (e.g., shrubs, herbs and mosses). So, we combined modeled soil respiration with modeled fixation and autotrophic respiration from understory PFTs for comparison against these chamber-measured net CO_2 fluxes. We also averaged net CO_2 flux measurements from all of the nine chambers for each half hour to accommodate the variations in those fluxes due to microtopography (e.g., hummock vs. hollow). Two half-hourly averaged values of net CO_2 fluxes were then aver-

aged again to obtain hourly mean net chamber CO_2 fluxes for comparison against modeled hourly sums of soil and understory fluxes averaged over modeled hummock and hollow. Model performance was evaluated from regression intercepts ($a \rightarrow 0$), slopes ($b \rightarrow 1$), coefficients of determination ($R^2 \rightarrow 1$), and root means squares for errors (RMSE $\rightarrow 0$) for each of 2005 and 2006.

3.2.5 Sensitivity of modeled peatland CO_2 exchange to artificial drainage

Large areas of northern boreal peatlands in Canada have been drained primarily for increased forest and agricultural production since plant productivity in pristine peatlands are known to be constrained by shallow WTD (Choi et al., 2007). Drainage and resultant WTD drawdown can affect both GPP and R_e on a short-term basis and the vegetation composition on a longer timescale, thereby changing overall net CO_2 exchange trajectories of a peatland. To predict the short-term effects of drainage on WTD and hence ecosystem net CO_2 exchange of WPL, we extended our simulation run into a projection run consisting of two 7-year cycles by using repeated weather sequences of 2003–2009. While doing so, we forced a stepwise drawdown in WTD_x by 1.0 and 2.0 m from that used in spin-up and simulation runs (Fig. 2) in the first (drainage cycle 1) and the second (drainage cycle 2) cycle, respectively. This projection run would give us a further insight into how the northern boreal peatland of western Canada would be affected by further WTD drawdown as a result of drier and warmer weather as well as a disturbance such as drainage. It would also provide us with a test of how sensitive the modeled C processes were to the changes in model lateral boundary condition as defined by WTD_x in ecosys.

4 Results

4.1 Model performance in simulating diurnal variations in ecosystem net CO_2 fluxes

Variations in precipitation can cause change in WTD and consequent variation in diurnal net CO_2 exchange across years. Ecosys simulated hourly EC-measured net CO_2 fluxes well from 2004 to 2009 with varying precipitation (Table 1). On a year-to-year basis, regressions of hourly modeled vs. EC-measured net ecosystem CO_2 fluxes gave intercepts within $0.1 \mu mol \, m^{-2} \, s^{-1}$ of 0 and slopes within 0.1 of 1, indicating minimal bias in modeled outputs during each year from 2004 to 2008 (Table 1a). On a growing season (May–August) basis, regressions of modeled on measured hourly net CO_2 fluxes yielded larger positive intercepts from 2004 to 2009 (Table 1b). The larger intercepts were predominantly caused by model overestimation of growing season daytime CO_2 fluxes. This overestimation was offset by model overestimation of nighttime CO_2 fluxes during the

winter, thus yielding smaller intercepts from throughout-the-year regressions of modeled vs. EC-measured fluxes (Table 1a vs. b). Values for coefficients of determination (R^2) were ~ 0.8 ($P < 0.001$) for all years from both throughout-the-year and growing season regressions (Table 1a, b). RMSEs were < 2.0 and $\sim 2.5 \mu mol \, m^{-2} \, s^{-1}$ for whole-year regressions from 2004 to 2008 (Table 1a) and for growing season regressions from 2004 to 2009 (Table 1b), respectively. Much of the variations in EC-measured CO_2 fluxes that were not explained by the modeled fluxes could be attributed to a random error of $\sim 20\%$ in EC methodology (Wesely and Hart, 1985). This attribution was further corroborated by root mean squares for random errors (RMSRE) in EC measurements, calculated for forests with similar CO_2 fluxes from Richardson et al. (2006), which were similar to RMSE (Table 1a, b). The similar values of RMSE and RMSRE also indicated that further constraint in model testing could not be achieved without further precision in EC measurements.

Regressions of modeled vs. chamber-measured net CO_2 fluxes gave R^2 of ~ 0.7 for ice-free periods (May–October) of 2005, and 2006 indicated that the variations in soil respiration and the fixation and aboveground autotrophic respiration due to WTD drawdown were modeled well (Table 1c). Smaller intercepts from those regressions meant lower model biases in simulating soil and understory CO_2 fluxes under a deepening WT (Table 1c). Although the slope was within 0.1 of one in 2005, it was a bit smaller in 2006. It indicated that the modeled soil and understory net CO_2 fluxes were smaller than the chamber-measured fluxes in 2006 (Table 1c). This was because some of the nighttime chamber fluxes in warmer nights of summer 2006 were as large as corresponding EC-measured net ecosystem CO_2 fluxes, which could not be modeled to their full extent. An RMSE lower than RMSRE meant that the errors in modeling soil and understory CO_2 fluxes were within the limit of random errors due to chamber measurements (Table 1c). It further indicated the robustness of modeled outputs for soil and understory CO_2 fluxes under different WTD conditions (e.g., shallower in 2005 vs. deeper in 2006) (Table 1c).

4.2 Seasonality in WTD and net ecosystem CO_2 exchange

Ecosys simulated the seasonal and interannual variations in WTD well from 2004 to 2009 at the WPL (Fig. 3b, d, f, h, j, l) (Mezbahuddin et al., 2016). Seasonality in net CO_2 exchange at the WPL was predominantly governed by that in temperature, which controlled the seasonality in phenology and GPP as well as that in R_e. Ecosys simulated the seasonality in phenology and hence GPP and R_e well during a gradual growing season WTD drawdown from 2004 to 2009, which was apparent by good agreements between modeled vs. EC gap-filled daily NEP (Fig. 3a, c, e, g, i, k) and modeled vs. EC-measured hourly net CO_2 fluxes (Table 1). Modeled NEPs throughout the winters of most of the years were

Table 1. Statistics from regressions between hourly modeled and measured net CO_2 fluxes from 2004 to 2009 at a western Canadian fen peatland.

(a) Regressions of modeled vs. EC-measured (recorded at $u^* > 0.15 \, \text{m s}^{-1}$) net ecosystem CO_2 fluxes over the whole years of 2004–2008*

Year	Total annual precipitation (mm)	n	a	b	R^2	RMSE ($\mu \text{mol m}^{-2} \text{s}^{-1}$)	RMSRE ($\mu \text{mol m}^{-2} \text{s}^{-1}$)
2004	553	5034	0.08 ± 0.03	1.10 ± 0.01	0.81	1.58	1.92
2005	387	5953	0.07 ± 0.03	1.03 ± 0.01	0.82	1.68	1.99
2006	465	6012	0.07 ± 0.03	1.08 ± 0.01	0.79	1.68	1.98
2007	431	5385	0.06 ± 0.03	0.99 ± 0.01	0.79	1.83	2.09
2008	494	5843	-0.01 ± 0.02	0.98 ± 0.01	0.84	1.63	2.02

(b) Regressions of modeled vs. EC-measured (recorded at $u^* > 0.15 \, \text{m s}^{-1}$) net ecosystem CO_2 fluxes over the growing seasons (May–August) of 2004–2009

Year	Total growing season precipitation (mm)	n	a	b	R^2	RMSE ($\mu \text{mol m}^{-2} \text{s}^{-1}$)	RMSRE ($\mu \text{mol m}^{-2} \text{s}^{-1}$)
2004	287	2043	0.55 ± 0.07	1.05 ± 0.01	0.78	2.27	2.55
2005	276	2200	0.82 ± 0.07	0.98 ± 0.01	0.79	2.50	2.74
2006	253	2107	0.48 ± 0.07	1.06 ± 0.01	0.78	2.36	2.76
2007	237	1822	0.65 ± 0.07	0.93 ± 0.01	0.75	2.91	3.06
2008	276	2070	0.32 ± 0.07	0.96 ± 0.01	0.82	2.45	2.85
2009	138	1870	0.76 ± 0.08	1.01 ± 0.01	0.81	2.27	2.83

(c) Regressions of modeled vs. measured chamber net CO_2 fluxes (understory vegetation and soil CO_2 fluxes) over ice-free periods (May–October) of 2005–2006

Year	Mean May–October WTD (m) Modeled	Measured	n	a	b	R^2	RMSE ($\mu \text{mol m}^{-2} \text{s}^{-1}$)	RMSRE ($\mu \text{mol m}^{-2} \text{s}^{-1}$)
2005	0.33	0.34	3285	0.43 ± 0.02	1.05 ± 0.01	0.68	1.19	2.38
2006	0.48	0.42	3855	0.31 ± 0.03	0.85 ± 0.01	0.71	1.44	3.25

WTD: water table depth below the hummock surface; (a, b) from simple linear regressions of modeled on measured ($\pm$ standard errors) and R^2: coefficient of determination; RMSE: root mean square for errors from simple linear regressions of measured on simulated; RMSRE: root mean square for random errors in measurements – RMSRE for eddy covariance (EC) measurements was estimated by inputting EC CO_2 fluxes recorded at u^* (friction velocity) $> 0.15 \, \text{m s}^{-1}$ into algorithms for the estimation of random errors due to EC CO_2 measurements developed for forests by Richardson et al. (2006); * whole-year modeled vs. EC net CO_2 flux regression for 2009 could not be done due to the lack of flux measurements from September to December in that year.

more negative than the EC gap-filled NEP, indicating larger modeled CO_2 effluxes than EC gap-filled fluxes during the winter (Fig. 3). The onset of photosynthesis at the WPL varied interannually depending upon spring temperature, which was also modeled well by ecosys. For instance, ecosys modeled a smaller early growing season (May) GPP and hence NEP in 2004, with a cooler spring than 2005, which was also apparent in daily EC gap-filled NEP (Fig. 3a vs. c).

4.3 WTD effects on diurnal net ecosystem CO_2 exchange

WTD variation can affect diurnal net CO_2 exchange by affecting peat O_2 status and consequently root and microbial O_2 and nutrient availability, growth and uptake, thereby in-fluencing CO_2 fixation and respiration. Ecosys simulated WTD effects on diurnal net CO_2 exchange at the WPL well over three 10-day periods with comparable weather conditions (radiation and air temperature) during the late growing seasons (August) of 2005, 2006 and 2008 (Fig. 4). A WTD drawdown from August 2005 to August 2006 in ecosys caused a reduction in peat water contents and a consequent increase in O_2 influxes from atmosphere into the peat that caused an increase in modeled soil CO_2 effluxes (Figs. 4c, 5c). This stimulation of soil respiration was corroborated by modeled vs. chamber-measured (Cai et al., 2010) nighttime soil CO_2 fluxes and understory aboveground autotrophic respiration (R_a) in August 2006 with a deeper WTD which were larger than those in 2005 with a shallower WTD (Fig. 5b).
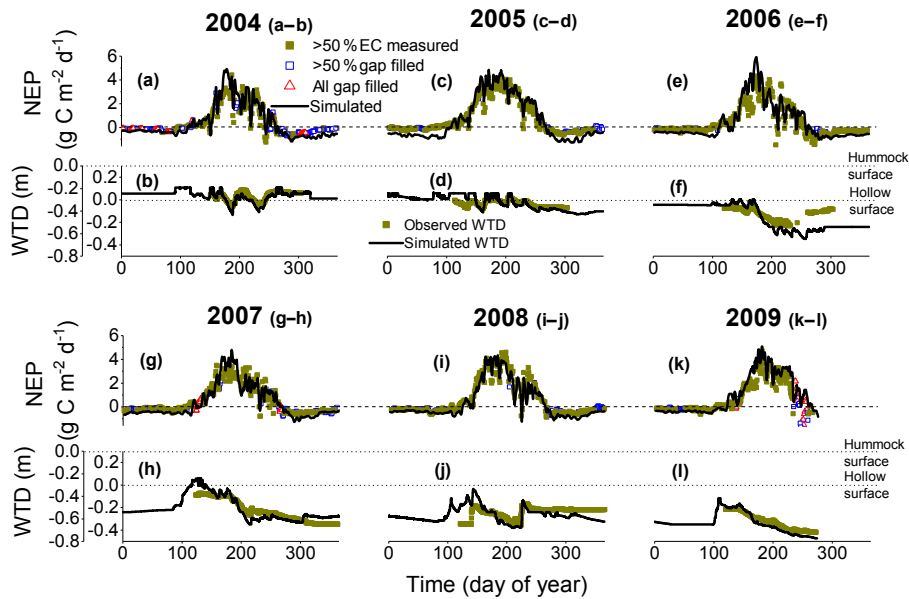
Figure 3. (a, c, e, g, i, k) Three-day moving averages of modeled and EC gap-filled (Flanagan and Syed, 2011) NEP and **(b, d, f, h, j, l)** hourly modeled and half-hourly measured (Syed et al., 2006; Cai et al., 2010; Long et al., 2010; Flanagan and Syed, 2011) WTD from 2004 to 2009 at a western Canadian fen peatland. A positive NEP means that the ecosystem is a carbon sink, and a negative NEP means that the ecosystem is a carbon source. A negative WTD represents a depth below hummock/hollow surface, and a positive WTD represents a depth above hummock/hollow surface.
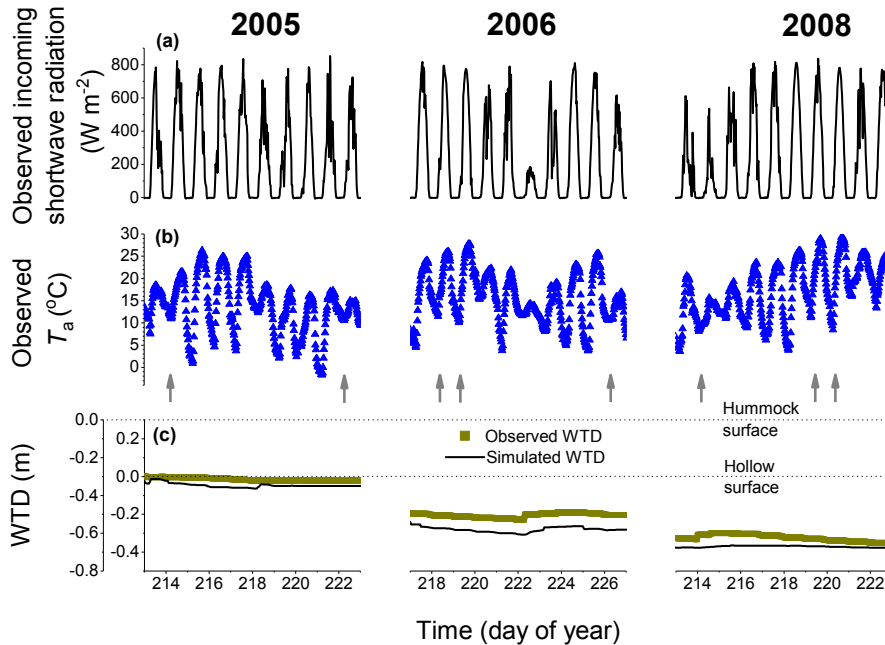
Figure 4. Half-hourly measured **(a)** incoming shortwave radiation and **(b)** T_a and **(c)** hourly modeled and half-hourly measured (Syed et al., 2006; Cai et al.; 2010, Long et al.; 2010, Flanagan and Syed, 2011) WTD during August of 2005, 2006 and 2008 at a western Canadian fen peatland. A negative WTD represents a depth below hummock/hollow surface, and a positive WTD represents a depth above hummock/hollow surface. Grey arrows indicate nights with similar temperatures.
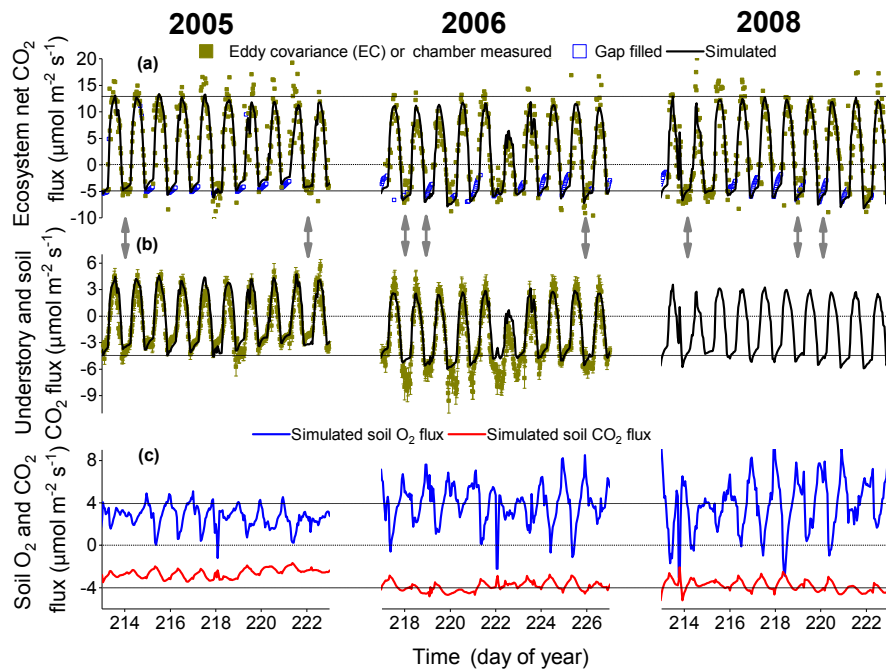
Figure 5. (a) Half-hourly EC-measured and gap-filled (Flanagan and Syed, 2011) and hourly modeled ecosystem net CO_2 fluxes, **(b)** half-hourly automated chamber-measured (Cai et al., 2010) and hourly modeled understory and soil CO_2 fluxes, and **(c)** hourly modeled soil CO_2 and O_2 fluxes during August of 2005, 2006 and 2008 at a western Canadian fen peatland. No chamber CO_2 flux measurement was available for 2008. Bars represent standard errors of means of chamber CO_2 fluxes ($n = 9$). A negative flux represents an upward flux or a flux out of the ecosystem, and a positive flux represents a downward flux or a flux into the ecosystem. Grey arrows indicate nights with similar temperatures in the same way as in Fig. 4.

Larger modeled soil CO_2 effluxes in 2006 contributed to the larger modeled ecosystem CO_2 effluxes (R_e) that were also apparent in nighttime EC CO_2 fluxes in 2006, which were larger than those in 2005 (Fig. 5a).

Continued WTD drawdown into the late growing season of 2008 (Fig. 4c) sustained improved peat oxygenation and hence larger modeled soil CO_2 effluxes (Fig. 5c). Consequently, modeled nighttime net ecosystem CO_2 fluxes and soil and understory CO_2 fluxes in 2006 and in 2008 were similarly larger than those in 2005, which was corroborated well by EC-measured nighttime fluxes during 2006 and 2008 vs. 2005 (Fig. 5a–b). Although nighttime modeled and EC-measured net ecosystem CO_2 fluxes in 2008 were larger than those in 2005, the daytime modeled and EC-measured CO_2 fluxes in 2008 did not decline with respect to those in 2005 (Fig. 5a). Similar daytime fluxes in 2005 and 2008 despite larger nighttime fluxes in 2008 than in 2005 indicated a greater late growing season CO_2 fixation in 2008 with a deeper WTD than in 2005 with a shallower WTD.

Beside WTD, temperature variation also profoundly affected ecosystem net CO_2 exchange at the WPL. For a given WTD condition, warmer weather raised R_e at the WPL as represented by larger modeled and measured ecosystem, soil and understory nighttime CO_2 fluxes in warmer nights than those in cooler nights (Figs. 4b and 5a–b). However, for

a given temperature modeled and EC-measured nighttime ecosystem CO_2 fluxes and modeled and chamber-measured nighttime soil and understory CO_2 fluxes were larger under deeper WT conditions in 2006 and 2008 than under shallower WT conditions in 2005 (denoted by the grey arrows in Figs. 4b and 5a–b). The nighttime CO_2 fluxes that were larger under deeper WTD than under shallower WTD with similar temperatures showed net a WTD drawdown effect on R_e (separated from the temperature effect) and hence on NEP.

The degree of R_e stimulation due to warming was also influenced by WTD at the WPL. The warming events in early to mid-August of 2006 and 2008, when the WT was deeper than in late July of 2005, caused gradual increases in modeled and EC- and chamber-measured nighttime ecosystem, soil and understory CO_2 effluxes (Fig. 6h, i, k, l). This R_e stimulation due to warming under a deeper WT contributed to declines in modeled and EC gap-filled July–August NEP in 2006 and 2008 (Fig. 3e, i). A lack of similar stimulation in R_e with warming under a shallower WT in 2005 did not yield a similarly evident stimulation of either modeled or measured ecosystem, soil and understory nighttime CO_2 effluxes (Fig. 6g, j vs. h, i, k, l), which resulted in the absence of a decline in July–August NEP in 2005 as occurred in 2006 and 2008 (Fig. 3c vs. e, i). Greater warming-driven R_e stim-
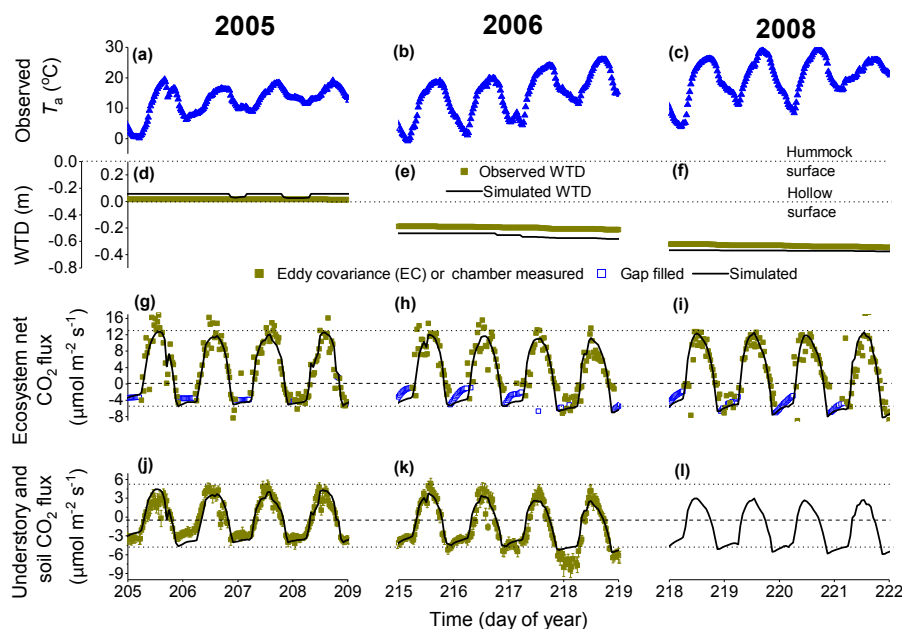
Figure 6. (a–c) Half-hourly observed T_a; **(d–f)** hourly modeled and half-hourly observed (Syed et al., 2006; Cai et al., 2010; Long et al., 2010; Flanagan and Syed, 2011) WTD; **(g–i)** half-hourly EC-measured and gap-filled (Flanagan and Syed, 2011) and hourly modeled ecosystem net CO_2 fluxes; **(j–l)** half-hourly automated chamber-measured (Cai et al., 2010) and hourly modeled understory and soil CO_2 fluxes during July–August of 2005, 2006 and 2008 at a western Canadian fen peatland. No chamber CO_2 flux measurement was available for 2008. Bars represent standard errors of means of chamber CO_2 fluxes ($n = 9$). A negative flux represents an upward flux or a flux out of the ecosystem, and a positive flux represents a downward flux or a flux into the ecosystem. A negative WTD represents a depth below hummock/hollow surface, and a positive WTD represents a depth above hummock/hollow surface

ulation under a deeper WT further indicated the importance of WTD in mediating potential effects of future warmer climates on boreal peatland NEP.

4.4 Interannual variations in WTD and net ecosystem productivity

The effects of WTD drawdown on modeled and EC gap-filled diurnal net ecosystem CO_2 exchange also contributed to the effects of interannual variation in WTD on that of NEP. Ecosys simulated the observed gradual drawdown of average growing season (May-August) WTD well from 2004 to 2009 (Fig. 7d) (Mezbahuddin et al., 2016). A small WTD drawdown caused a large increase in both modeled and EC-derived growing season GPP from 2004 to 2005 (Fig. 7b). This increase in GPP was also contributed by a larger GPP in May 2005, which was warmer than May 2004. This small WTD drawdown, however, did not raise either modeled or EC-derived growing season R_e from 2004 to 2005 (Fig. 7c). June and July of 2005 were cooler than 2004 by over $2\,°C$, which caused cooler soil that reduced R_e in 2005. The reduction in R_e in June–July 2005 due to cooler soil more than fully offset the increase in R_e due to the small WTD drawdown and resulted in modeled and EC-derived growing season R_e values that were smaller in 2005 than in 2004 (Fig. 7c). Larger GPP along with smaller R_e in 2005 con-

tributed to larger modeled and EC gap-filled growing season NEP in 2005 than in 2004 (Fig. 7a).

WTD drawdown from 2005 to 2006 raised both modeled and EC-derived growing season GPP and R_e (Fig. 7b, c, d). A warmer growing season in 2006 caused warmer soil that further contributed to the increase in modeled and EC-derived growing season R_e from 2005 with a shallower WT to 2006 with a deeper WT (Figs. 5, 6 and 7c, d). An increase in growing season R_e that was greater than the increase in growing season GPP caused a decline in modeled and EC-derived growing season NEP from 2005 to 2006 (Fig. 7a). Continued growing season WTD drawdown from 2006 to 2008 caused similar increases in modeled growing season GPP and R_e and hence caused no significant change in modeled growing season NEP (Fig. 7a–d). With this continued WTD drawdown from 2006 to 2008, however, EC-derived growing season GPP increased more than EC-derived growing season R_e, which resulted in a larger EC-derived NEP in the growing season of 2008 than in 2006 (Fig. 7a–d). A further growing season WTD drawdown from 2008 to 2009 caused reductions in both modeled and EC-derived growing season GPP and R_e (Fig. 7a–d). Reductions in GPP and R_e from 2008 to 2009 were also contributed by lower T_a in 2009 than in 2008, which caused cooler canopies and soil (Fig. 7b–d). The reduction in EC-derived growing season GPP was larger than that in EC-derived growing season R_e, thereby causing
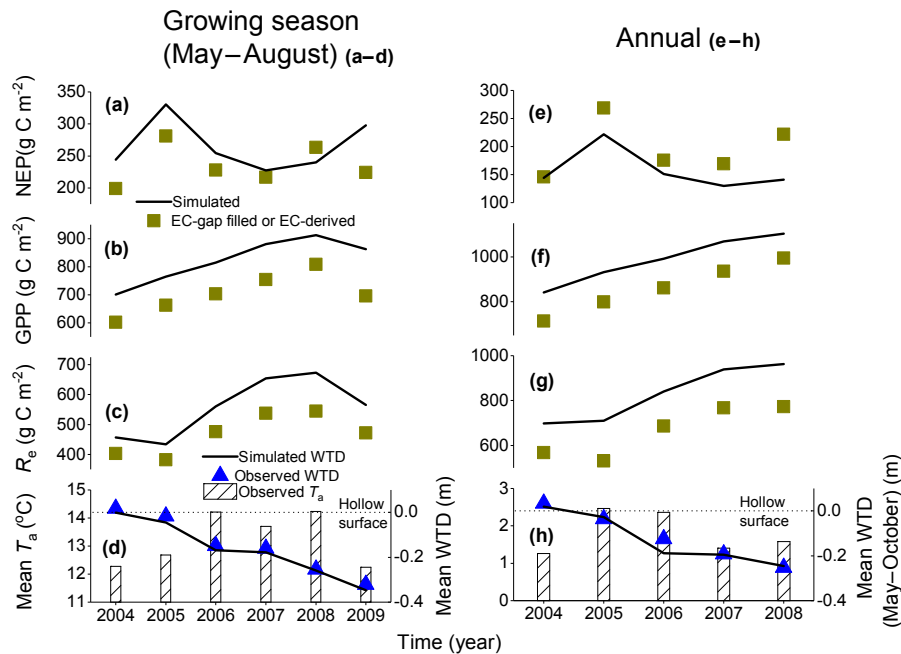
Figure 7. Modeled and EC-derived (Flanagan and Syed, 2011) growing season (May–August) sums of **(a)** NEP, **(b)** GPP and **(c)** R_e during 2004–2009; **(d)** observed mean growing season T_a and measured and modeled average growing season WTD during 2004–2009; modeled and EC-derived (Flanagan and Syed, 2011) annual sums of **(e)** NEP, **(f)** GPP and **(g)** R_e during 2004–2008 and **(h)** observed mean annual T_a and measured and modeled average WTD during ice-free periods (May–October) of 2004-2008 at a western Canadian fen peatland. A negative WTD represents a depth below hollow surface, and a positive WTD represents a depth above hollow surface. A positive NEP means that the ecosystem is a carbon sink. Annual modeled vs. EC gap-filled NEP, GPP and R_e estimates for 2009 were not compared due to the lack of flux measurements from September to December in that year.

a decrease in growing season EC gap-filled NEP from 2008 to 2009 (Fig. 7a–c). By contrast, the reduction in modeled growing season GPP was smaller than the reduction in modeled R_e that yielded an increase in modeled growing season NEP from 2008 to 2009 (Fig. 7a–c).

Modeled and EC-derived growing season GPP and R_e in 2009 were larger than those in 2004 despite similar mean T_a in those years (Fig. 7a–d). It suggested that increases in growing season GPP and R_e from 2004 to 2009 was a net effect of the deepening of average growing season WT (Fig. 7a–d). It was further corroborated by polynomial regressions of modeled growing season GPP and R_e against modeled average growing season WTD and by similar regressions of EC-derived growing season GPP and R_e against site-measured average growing season WTD (Fig. 8b, c). These relationships showed that there were increases in modeled and EC-derived growing season GPP and R_e with a deepening of the growing season WT from 2004 to 2008, after which further WTD drawdown in 2009 started to cause slight declines in both GPP and R_e (Fig. 8b, c). Neither modeled nor EC gap-filled growing season NEP yielded significant regressions when regressed against modeled and measured growing season WTD, respectively (Fig. 8a). It indicated that similar increases in modeled and EC-derived growing season GPP and R_e with a deepening of the WT had

no net effects of WTD drawdown on either modeled or EC-derived growing season NEP (Figs. 7a–d and 8a).

Similar to the growing season trend, drawdown of both measured and modeled WTD averaged over the ice-free periods (May–October) from 2004 to 2008 stimulated modeled and EC-derived annual GPP and R_e (Figs. 7f, g, h and 8e, f). Similar increases in both modeled and EC-derived annual GPP and R_e with WTD drawdown had no net WTD effects on modeled and EC gap-filled annual NEP (Figs. 7e, 8d). Although modeled WTD effects on GPP, R_e and hence NEP were corroborated well by EC-derived GPP, R_e and EC gap-filled NEP, the modeled values for growing season and annual GPP and R_e were consistently larger than the EC-derived GPP and R_e throughout the study period (Figs. 7b, c, f, g and 8b, c, e, f).

Increased GPP with WTD drawdown (Figs. 7b, f and 8b, e) was modeled predominantly through increased root growth and uptake of nutrients and consequently improved leaf nutrient status and hence more rapid CO_2 fixation in vascular PFTs. Under a shallow WT during the growing season of 2004, roots in modeled black spruce and tamarack PFTs hardly grew below 0.35 m from the hummock surface. Modeled root densities of both black spruce and tamarack were higher by 2–3 orders of magnitude in the top 0.19 m of the hummock (data not shown). A WTD drawdown by 0.35 m

Table 2. Effects of WTD drawdown on components of ecosystem carbon and nutrient cycles of a western Canadian fen peatland.

		Modeled	Eddy-covariance-derived/ biometrically measured at the site[a]	Values from other studies in similar peatlands
Growing season (May to August) mean WTD drawdown from 2004 to 2009		from 0.3 m below the hummock surface (at the hollow surface) in 2004 to 0.65 m below the hollow surface (0.35 below the hollow surface) in 2009	from 0.32 m below the hummock surface (0.02 m below the hollow surface) in 2004 to 0.62 m below the hummock surface (0.32 m below the hollow surface) in 2009	
Rate of increase in R_e with each 0.1 m of WTD drawdown		$0.26\ \mu\text{mol CO}_2\ \text{m}^{-2}\ \text{s}^{-1}$	$0.16\ \mu\text{mol CO}_2\ \text{m}^{-2}\ \text{s}^{-1}$	$0.32 \pm 0.27\ \mu\text{mol CO}_2\ \text{m}^{-2}\ \text{s}^{-1}$ [b]
Rate of increase in GPP with each 0.1 m WTD drawdown		$0.39\ \mu\text{mol CO}_2\ \text{m}^{-2}\ \text{s}^{-1}$	$0.22\ \mu\text{mol CO}_2\ \text{m}^{-2}\ \text{s}^{-1}$	(1) $0.32 \pm 0.15\ \mu\text{mol CO}_2\ \text{m}^{-2}\ \text{s}^{-1}$ [b]; (2) $0.47 \pm 0.06\ \mu\text{mol CO}_2\ \text{m}^{-2}\ \text{s}^{-1}$ [c]
Leaf nitrogen concentration (mid-July 2004)	black spruce	$14.3\ \text{g N kg}^{-1}\ \text{C}$	$12.4 \pm 0.6\ \text{g N kg}^{-1}\ \text{C}$	
	tamarack	$32.1\ \text{g N kg}^{-1}\ \text{C}$	$32.6 \pm 1.4\ \text{g N kg}^{-1}\ \text{C}$	
	dwarf birch	$37.4\ \text{g N kg}^{-1}\ \text{C}$	$41.4 \pm 1.8\ \text{g N kg}^{-1}\ \text{C}$	
Leaf nitrogen (N) to phosphorus (P) ratio (mid-July 2004)	black spruce	6.6:1	7.1:1	
	tamarack	5.2:1	6.3:1	
	dwarf birch	4.8:1		
Increase in foliar nitrogen concentrations with WTD drawdown	black spruce	from 14.3 to 17.2 g N kg^{-1} C with the growing season WTD drawdown from 0.3 m below the hummock surface in 2004 to 0.65 m below the hummock surface in 2009		(1) from 20.8 ± 0.6 to 27 ± 0.4 g N kg^{-1} C with a WTD drawdown from 0.24 to 0.7 m below peat surface [d]; (2) from 18.7 ± 0.05 to 21.3 ± 0.06 g N kg^{-1} C for a WTD drawdown of 0.4–0.5 m [e]
	tamarack	from 32.1 to 36.7 g N kg^{-1} C with the growing season WTD drawdown from 0.3 m below the hummock surface in 2004 to 0.65 m below the hummock surface in 2009		(1) from 41.4 ± 0.4 to 66.2 ± 1.2 g N kg^{-1} C for a WTD drawdown from 0.24 to 0.7 m below peat surface [d]; (2) from 35.9 ± 0.1 to 41.7 ± 0.18 g N kg^{-1} C for a WTD drawdown of 0.4–0.5 m [e]
	dwarf birch	from 37.4 to 45.1 g N kg^{-1} C with the growing season WTD drawdown from 0.3 m below the hummock surface in 2004 to 0.65 m below the hummock surface in 2009		
Increase in maximum rooting depth with WTD drawdown	black spruce	from 0.35 to 0.65 m below the hummock surface with the growing season WTD drawdown from 0.3 m below the hummock surface in 2004 to 0.65 m below the hummock surface in 2009		from 0.1 to 0.6 m below hummock surface with a WTD drawdown from 0.1 to 0.7 m below hummock surface [f]
	tamarack	from 0.35 to 0.65 m below the hummock surface with the growing season WTD drawdown from 0.3 m below the hummock surface in 2004 to 0.65 m below the hummock surface in 2009		from 0.2 to 0.6 m below hummock surface with a WTD drawdown from 0.1 to 0.6 m below hummock surface [f]

[a] Syed et al. (2006), Flanagan and Syed (2011). [b] Peichl et al. (2012) for a Michigan fen peatland complex that has similar peat and plant functional types as our study site. [c] Ballantyne et al. (2014) for a Swedish fen. [d] Choi et al. (2007) for a central Alberta fen peatland located ∼350 km to the southwest of the study site. [e] Macdonald and Lieffers (1990) for a northern Alberta fen peatland located ∼250 km to the northwest of the study site. [f] Lieffers and Rothwell (1987) for a northern Alberta fen peatland located ∼250 km to the northwest of the study site. [a, d, e] unit conversions for leaf nutrient values were done by assuming organic C as 50 % of total leaf dry matter.
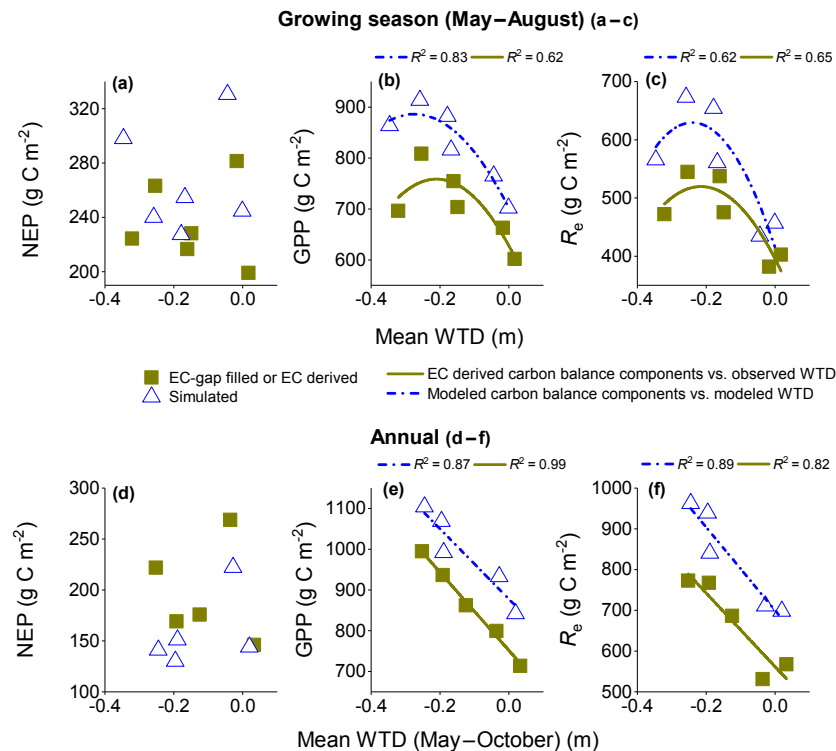
Figure 8. Regressions ($P < 0.001$) of growing season (May–August) sums of modeled and EC-derived (Flanagan and Syed, 2011) **(a)** NEP, **(b)** GPP and **(c)** R_e on growing season averages of modeled and observed WTD during 2004–2009; regressions ($P < 0.001$) of annual sums of modeled and EC-derived (Flanagan and Syed, 2011) **(d)** NEP, **(e)** GPP and **(f)** R_e on average modeled and measured WTD during ice-free periods (May–October) of 2004–2008 at a western Canadian fen peatland. A negative WTD represents a depth below hollow surface, and a positive WTD represents a depth above hollow surface. A positive NEP means that the ecosystem is a carbon sink.

from the growing season of 2004 to that of 2009 caused an increase in maximum modeled rooting depth in both PFTs (Table 2). Increased root growth in modeled vascular PFTs augmented root surface area for nutrient uptake under a deeper WT in the growing season of 2009 than in 2004. Increased root surface area along with increased nutrient availability due to more rapid mineralization with improved aeration as a result of WTD drawdown from 2004 to 2009 caused improved root nutrient uptake in modeled vascular PFTs. Increased root growth, nutrient availability and hence uptake due to WTD drawdown from the growing season of 2004 to that of 2009 caused an increase in modeled foliar N concentrations in black spruce, tamarack and dwarf birch PFTs driving the increases in GPP modeled over this period (Figs. 7b, f and 8b, e) (Table 2).

4.5 Simulated drainage effects on WTD and NEP

Artificial drainage can drastically alter WTD in a peatland that can cause dramatic changes in peatland NEP by shifting the balance between GPP and R_e. Projected growing season WT was deeper by ~ 0.5 m and ~ 0.55 m, respectively, from those in the real-time simulation in drainage cycles 1 and 2 in all the years from 2004 to 2009 (Fig. 9a). Modeled

growing season GPP increased with drainage-induced WTD drawdown up to ~ 0.5 m below the hollow surface (~ 0.8 m below the hummock surface), below which GPP decreased (Fig. 9c, f). The WTD drawdown affected modeled vascular and nonvascular growing season GPP quite differently. Modeled growing season vascular GPP increased with WTD drawdown before it plateaued and eventually decreased when WTD fell below ~ 0.6 m from the hollow surface (~ 0.9 m below the hummock surface) (Fig. 10a, c, e). By contrast, modeled nonvascular growing season GPP continued to decrease with WTD drawdown below ~ 0.1 m from the hollow surface (~ 0.4 m below the hummock surface) (Fig. 10a, b, d).

WTD drawdown due to simulated drainage not only affected modeled growing season GPP but also affected, and was affected by, the associated change in transpiration from vascular canopies. Deeper WTD_x in drainage cycle 1 caused larger hydraulic gradients and greater lateral discharge, thereby deepening the WT with respect to that in the real-time simulation (Fig. 9a). Larger GPP in the drainage cycle 1 than in the real-time simulation throughout the growing seasons of 2004–2007 caused a greater vertical water loss through rapid transpiration from vascular canopies that
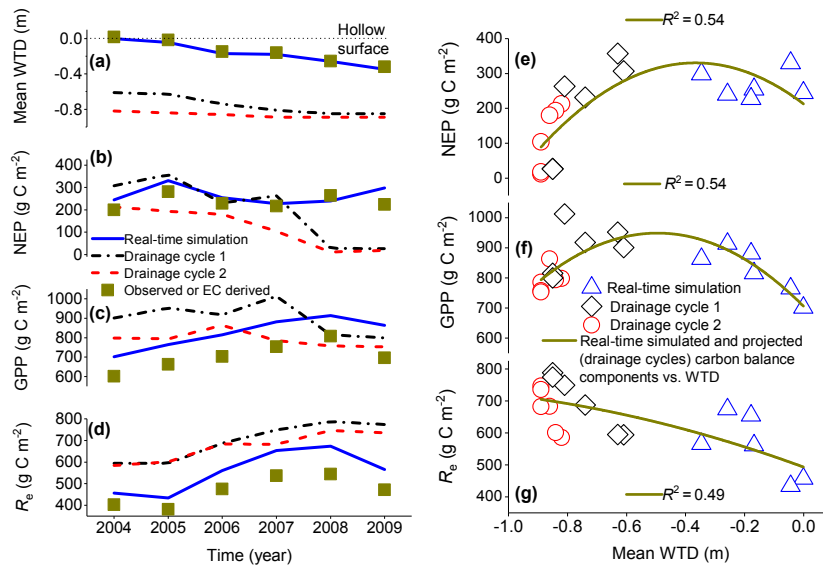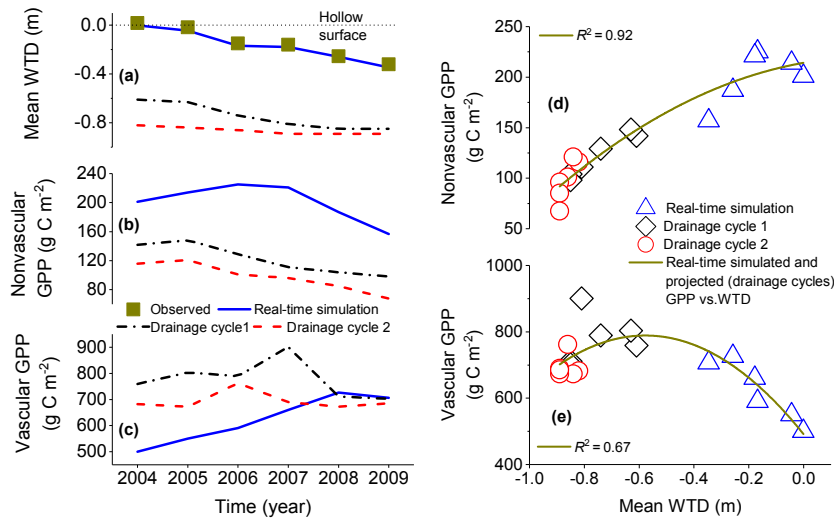
Figure 9. (a) Observed, simulated (real-time simulation) and projected (drainage cycles 1 and 2) average growing season (May-August) WTD; EC-derived, simulated and projected growing season sums of **(b)** NEP, **(c)** GPP and **(d)** R_e; and regressions ($P < 0.001$) of simulated and projected sums of **(e)** NEP, **(f)** GPP and **(g)** R_e on simulated and projected average growing season WTD during 2004–2009 at a western Canadian fen peatland. A negative WTD represents a depth below hollow surface, and a positive WTD represents a depth above hollow surface. A positive NEP means that the ecosystem is a C sink.

Figure 10. Simulated (real-time simulation) and projected (drainage cycles 1 and 2) **(a)** average growing season (May–August) WTD, **(b)** growing season sums of nonvascular (moss) GPP and **(c)** growing season sums of vascular GPP; regressions ($P < 0.001$) of simulated and projected sums of **(d)** nonvascular GPP and **(e)** vascular GPP on simulated and projected average growing season WTD during 2004–2009 at a western Canadian fen peatland. A negative WTD represents a depth below hollow surface, and a positive WTD represents a depth above hollow surface.

further contributed to this deepening of the WT (Fig. 9c). However, greater lateral water discharge in drainage cycle 2 caused by deeper WTD_x did not deepen the modeled growing season WT much below that in cycle 1 (Fig. 9a). The larger lateral water loss through discharge in drainage cycle 2 than in cycle 1 was mostly offset by slower vertical wa-

ter losses due to vascular plant water stress as indicated by smaller GPP in the drainage cycle 2 (Fig. 9c). The changing feedbacks between WTD, and GPP and plant water relations in ecosys also indicated the ability of the model to simulate hydrological self-regulation which is an important characteristic of peatland eco-hydrology (Dise, 2009).

Modeled growing season R_e continued to increase with projected drainage-driven WTD drawdown (Fig. 9d, g). Reductions in modeled growing season R_e from drainage cycle 1 to 2 during 2006–2009 indicated R_e inhibition due to desiccation of near-surface peat layers and surface residues (Fig. 9d). Overall GPP increased more than R_e with drainage-driven initial WTD drawdown that caused a small increase in modeled growing season NEP (Fig. 9 b, e). Continued drainage-driven WTD drawdown, however, caused declines in GPP particularly in the model years of 2008 and 2009 (Fig. 9c). This decrease in GPP was also accompanied by increased R_e, thereby causing a decrease in NEP when the WT fell below a threshold of about ~ 0.45 m from the hollow surface, particularly during the drier years (Fig. 9b–g). This projected drainage effect on WTD and NEP may be transient. Long-term manipulation of WTD may produce different trajectories of WTD effects on C processes and plant water relations in northern boreal peatlands via vegetation adaptation and succession (Strack et al., 2006; Munir et al., 2014).

5　Discussion

5.1　Modeling WTD effects on northern boreal peatland NEP

Hourly modeled and measured net ecosystem, soil and understory CO_2 fluxes, and modeled and EC-derived seasonal and annual NEP, GPP and R_e showed that WTD drawdown raised both GPP and R_e at the WPL (Figs. 3–8). Similar increases in GPP and R_e with WTD drawdown yielded no net effect of WTD drawdown on NEP at the WPL during 2004–2009 (Figs. 7–8). Our hypotheses, which outlined how coupled eco-hydrology and biogeochemistry algorithms in ecosys would simulate and explain the mechanisms of these WTD effects on R_e, GPP and NEP at this boreal fen, are examined in details in the following Sect. of 5.1.1 to 5.1.4.

5.1.1　Hypothesis 1: increase in R_e with WTD drawdown

Shallow WTD in ecosys caused a shallow aerobic zone above the WT and a thicker anaerobic zone below the WT. In the shallow aerobic zone, peat O_2 concentration $[O_{2s}]$ was well above the Michaelis–Menten constant for O_2 reduction ($K_m = 0.064$ g m^{-3}), and hence DOC oxidation and consequent microbial uptake and growth in ecosys were not much limited by $[O_{2s}]$ (Eqs. SA17a, SC14c). On the contrary, $[O_{2s}]$ in the thicker anaerobic zone below the WT was well below K_m so that DOC oxidation was coupled with DOC reduction by anaerobic heterotrophic fermenters, which yielded much less energy (4.4 kJ g^{-1}C) than did DOC oxidation coupled with O_2 reduction (37.5 kJ g^{-1}C) (Fig. 1) (Eq. SA21). Lower energy yields in the thicker anaerobic zone caused slower microbial growth (Eq. SA25) and R_h (Eq. SA13). Since the

anaerobic zone in ecosys was thicker than the aerobic zone under a shallow WT, smaller R_h modeled in the anaerobic zone contributed to reduced modeled soil respiration and hence R_e which was corroborated by EC and chamber measurements at the WPL (Figs. 5–8) (Tables 1 and 2).

WTD drawdown in ecosys caused peat pore drainage and increased θ_g, thereby deepening the aerobic zone. It raised D_g (Eq. SD44) and increased O_2 influxes into the peat (Fig. 5c) (Eqs. SD42–SD43). Increased O_2 influxes enhanced $[O_{2s}]$ and stimulated R_h (Eqs. SA13, SA20), soil respiration and hence R_e (Figs. 5–8). Rapid mineralization of DON and DOP due to improved $[O_{2s}]$ under a deeper WT also raised aqueous concentrations of NH_4^+, NO_3^- and $H_2PO_4^-$ (Eqs. SC23a, c, e), which increased microbial nutrient availability, uptake (Eq. SA22) and growth (Eq. SA29) and enhanced R_e further (Fig. 1) (Figs. 5–8). Modeled R_e stimulation by improved peat oxygenation due to WTD drawdown was corroborated well by EC and chamber measurements at the site (Figs. 5–8) (Tables 1 and 2). Although the modeled rate of increase in R_e with each 0.1 m of WTD drawdown was larger than the EC-derived rate, it is still comparable to rates reported for other similar peatlands (Table 2). Kotowska (2013) carried out chamber-based field measurements and laboratory incubation experiments in a moderately rich fen very close to our study site; she reported that a WTD drawdown-driven stimulation of aerobic microbial decomposition contributed to increased R_e. Mäkiranta et al. (2009) also found rapid microbial decomposition in a Finish peatland due to a thicker aerobic zone and consequently larger amounts of decomposable organic matter exposed to aerobic oxidation.

Apart from WTD, peat warming in ecosys also increased rates of decomposition (Eq. SA1) through an Arrhenius function (Eq. SA6) and hence raised R_h and R_e (Figs. 4–7). The warming effect on decomposition in ecosys was also modified by WTD. For a similar warming, greater thermal diffusivity in peat with a deeper WT and consequent smaller water contents caused greater peat warming (Eqs. SD34, SD36). It enabled larger simulation of R_e during warming periods in 2006 and 2008 with a deeper WT than in 2005 (Fig. 6). Increased stimulation of peat decomposition by warming under a deeper WT was also modeled by Grant et al. (2012) using the same model, ecosys, over a northern fen peatland at Wisconsin, USA, and by Ise et al. (2008) using a land surface scheme named ED-RAMS (Ecosystem Demography Model version 2 integrated with the Regional Atmospheric Modeling System) coupled with a soil biogeochemical model across several shallow and deep peat deposits in Manitoba, Canada.

5.1.2　Hypothesis 2: increase in GPP with WTD drawdown

Modeled WTD variations influenced GPP by controlling root and microbial O_2 availability, energy yields, root and mi-

crobial growth and decomposition, rates of mineralization, and hence root nutrient (nitrogen) availability and uptake (Fig. 1). Wet soils under a shallow WT caused low O_2 diffusion (Fig. 5c) (Eqs. SD42–SD44) into the peat, and consequent low $[O_{2s}]$ meant that root O_2 demand had to be mostly met by $[O_{2r}]$. Ecosys inputs for root porosity ($\theta_{pr} = 0.1$) that governed O_2 transport through aerenchyma (Eq. SD45) and hence maintained $[O_{2r}]$ were not enough to meet the root O_2 demand in saturated soil by the two overstory tree PFTs, i.e., black spruce and tamarack, causing shallow root systems to be simulated in these two tree PFTs under shallow WTD (Sect. 4.4). The understory shrub PFT (dwarf birch) had a higher root porosity ($\theta_{pr} = 0.3$) and hence had deeper rooting under a shallow WT than the two tree PFTs. Shallow rooting in the tree PFTs reduced root surface area for nutrient (nitrogen) uptake. Root nutrient (nitrogen) uptake (Eqs. SC23b, d, f) in all the PFTs was also constrained by low nitrogen availability due to smaller aqueous concentrations of NH_4^+ and NO_3^- (Eqs. SC23a, c, e) resulting from slower mineralization (Eq. SA26) of DON (Eq. SA7) because of low $[O_{2s}]$ in the wet soils under a shallow WT (Fig. 1). Slower root growth and nutrient (nitrogen) uptake caused lower foliar σ_N with respect to foliar σ_C (Eq. SC11) that slowed the rates of carboxylation (Eq. SC6) and hence reduced vascular GPP (Eq. SC1) under a shallow WT.

WTD drawdown enhanced O_2 diffusion (Fig. 5c) (Eqs. SD42–SD44) and raised $[O_{2s}]$ so that root O_2 demand in all the three vascular PFTs was almost entirely met by $[O_{2s}]$. Consequently roots in all the PFTs could grow deeper, which increased the root surface for nutrient (nitrogen) uptake (Table 2) (Sect. 4.4). An increase in modeled rooting depth due to WTD drawdown was corroborated well by studies on same PFTs grown on similar peatlands very close to our study site (Table 2). Murphy et al. (2009) found a significant increase in tree fine-root production with WTD drawdown by 0.15–0.2 m during a WTD manipulation study in a Finish peatland. Beside improved root growth, greater $[O_{2s}]$ under a deeper WT also enhanced rates of mineralization (Eq. SA26) of DON (Eq. SA7), which raised aqueous concentrations of NH_4^+ and NO_3^- and hence facilitated root nutrient (nitrogen) availability and uptake (Fig. 1). Enhanced root nutrient (nitrogen) uptake increased foliar σ_N with respect to foliar σ_C (Eq. SC11), which hastened the rates of carboxylation (Eq. SC6) and hence raised vascular GPP (Eq. SC1) under a deeper WT.

The three modeled vascular PFT were predominantly N limited as indicated by mass-based modeled foliar N-to-P ratios that matched well with site-measured mass-based foliar N-to-P ratios (Table 2). Mass-based modeled and measured foliar N-to-P ratios in all the PFTs were less than 16 : 1, indicating that the vegetation at the WPL was N limited (Aerts and Chapin III, 1999). Since the modeled PFTs were predominantly N limited, increases in foliar N concentrations as a result of improved root growth and root nitrogen availability and uptake with WTD drawdown enhanced modeled

carboxylation rates and hence modeled GPP. In a similar fen peatland close to our study site, Choi et al. (2007) found an increase in peat NO_3^--N due to enhanced nitrogen mineralization and nitrification stimulated by a WTD drawdown, which improved foliar N status and hence increased radial tree growth of black spruce and tamarack trees (Table 2). Macdonald and Lieffers (1990) also found improved foliar N concentrations in black spruce and tamarack trees that enhanced net photosynthetic C assimilation rates by those tree species in a northern Alberta moderately rich fen (Table 2). The rates of increases in foliar N concentrations in black spruce and tamarack trees due to WTD drawdown as reported in those studies are comparable to those in our modeled outputs (Table 2). Although the modeled rate of increase in GPP with each 0.1 m of WTD drawdown was larger than the EC-derived rate, it is still comparable to rates reported for other similar peatlands (Table 2).

5.1.3 Hypothesis 3: microbial water stress on R_e due to WT deepening below a threshold WTD

When modeled WTD fell below a threshold of ~ 0.3 m from the hollow surface (~ 0.6 m below the hummock surface), the desiccation of the surface residue layer and near-surface shallow peat layers reduced microbial access to substrate for decomposition (Eq. SA15), which enabled the simulation of reduced R_h in those layers. When reduction in surface residue and near-surface R_h more than fully offset the increase in deeper R_h, net ecosystem R_h decreased. The offsetting effect on R_h partly contributed to a simulated decrease in growing season R_e ($= R_h + R_a$) from 2008 to 2009 with a WTD drawdown that was corroborated by a similar decrease in EC-derived R_e (Fig. 7c). Greater reductions in R_h in desiccated surface residue and near-surface peat layers also caused the reductions in growing season R_e in drainage cycle 2 from those in cycle 1 during 2007–2009 in the projected drainage simulation (Fig. 9d). Similar to our study, Peichl et al. (2014) found reductions in R_e when WTD fell below a threshold of 0.25 m from the peat surface in a Swedish fen, which could be partially attributed to a reduction in near-surface R_h due to desiccation. Mettrop et al. (2014) in a controlled incubation experiment found that the rates of microbial respiration in a nutrient-rich Dutch fen had initially increased with peat drying and consequent improved aeration before excessive drying and consequent peat desiccation reduced microbial respiration efficiency, growth and biomass. While modeling the CO_2 exchange of a northern temperate bog using ecosys, Dimitrov et al. (2010a) found that a decrease in desiccated near-surface peat respiration partially offset increased deeper peat respiration when the WT deepened below a threshold of 0.6–0.7 m from the hummock surface.

5.1.4 Hypothesis 4: plant water stress on GPP due to WT deepening below a threshold WTD

The desiccation of near-surface peat layers with WTD drawdown below a threshold level also caused reduced plant water uptake from those layers which were colonized by most of the vascular root systems and all of the belowground biomasses of nonvascular mosses (Eqs. SD9–SD29). When WTD fell below ~ 0.1 m from the hollow surface (~ 0.4 m below the hummock surface), vertical recharge through capillary rise from the WT was not adequate to maintain near-surface peat moisture. It reduced peat ψ_s and raised peat Ω_s (Eq. SB9), which suppressed root and moss water uptake (U_w) (Eq. SB6) from desiccated near-surface peat layers (Fig. 1). Since moss U_w entirely depended upon moisture supply from the near-surface layers, a reduction in U_w from the desiccation of these layers caused a reduction in moss ψ_c and hence moss GPP (Fig. 1) (Eqs. SC1, SC4) (Mezbahuddin et al., 2016). A reduction in root U_w from desiccated near-surface layers, however, was offset by increased root U_w (Eq. SB6) from deeper wetter layers, which had higher ψ_s and lower Ω_s, due to deeper root growth facilitated by enhanced aeration. It enabled the vascular PFTs in ecosys to sustain ψ_c, canopy ψ_t (Eq. SB4), g_c (Eqs. SB2, SC4) and hence to sustain increased GPP (Eq. SC1) due to higher root nutrient (nitrogen) availability and uptake (Fig. 1) (Mezbahuddin et al., 2016). Increased vascular GPP and consequent greater vascular plant growth further imposed limitations of water, nutrient and light on the modeled nonvascular PFTs due to interspecific competition and greater shading from the overstory vascular PFTs. However, an increases in vascular GPP due to enhanced plant nutrient (nitrogen) status more than fully offset the suppression in moss GPP due to moss drying and greater shading and competition from the overstory, thereby causing a net increase in modeled GPP with WTD drawdown (Figs. 7b and 10b, c). This simulation of increased vascular dominance over moss with a deepening of the WT was corroborated by several WTD manipulation studies (e.g., Moore et al., 2006, Munir et al., 2014) in similar peatlands in Alberta that reported increased tree, shrub and herb growths over mosses with WTD drawdown. However, an increase in projected vascular GPP eventually plateaued, and GPP started to decline when the WT fell below ~ 0.6 m from the hollow surface (~ 0.9 m below the hummock surface) (Figs. 10c, e). This was because deeper root U_w (Eq. SB6) could no longer offset the suppression of near-surface root U_w when the WT fell below threshold WTD, thereby causing lower ψ_c, ψ_t (Eq. SB4), g_c (Eqs. SB2, SC4) and slower CO_2 fixation (Eq. SC6) (Fig. 1).

These threshold WTD effects on modeled vascular and nonvascular plant water relations were validated well by testing modeled vs. site-measured hourly energy fluxes (latent and sensible heat) and Bowen ratios and modeled vs. site-measured daily peat moisture at different depths throughout 2004–2009 as described in Mezbahuddin et al. (2016). Ri-

utta et al. (2007) measured a reduction in moss productivity due to water limitation when WTD fell below ~ 0.15 m from the surface in a Finish fen peatland. However, they reported a sustained vascular GPP during that period, indicating no vascular water stress (Riutta et al., 2007). Peichl et al. (2014) reported a reduction in moss GPP due to moss drying caused by an insufficient moisture supply through capillary rise when WTD fell below 0.25 m from the surface in a Swedish fen. Reductions in moss GPP due to decreased moss canopy water potentials were also modeled by Dimitrov et al. (2011) using the same model, ecosys, when WTD fell below 0.3 m from the hummock surface of a Canadian temperate bog. They, however, found no vascular plant water stress and hence no reduction in vascular GPP during that period. Similarly, Kuiper et al. (2014) found reductions in moss productivity with peat drying while vascular productivity was sustained in a simulated drought experiment on a Danish peat.

Continued deepening of the WT can also cause vascular plant water stress and hence reductions in vascular GPP as projected in our drainage simulation (Fig. 10c, e). This can also be corroborated by field measurements across various northern boreal fen peatlands in Canada and Sweden. Sonnentag et al. (2010) found a reduction in g_c of a canopy that included tamarack and dwarf birch and a consequent decline in GPP when the WT fell below 0.3 m from the ridge surface at a fen peatland in Saskatchewan. Peichl et al. (2014) also found a reduction in vascular GPP due to plant water stress when WTD fell below 0.25 m from the surface in a Swedish fen. The WTD threshold for reductions in vascular GPP in those two field studies were shallower than that in our modeled projection, i.e., ~ 0.6 m from the hollow surface (~ 0.9 m below the hummock surface) (Fig. 10a, c, e), thereby indicating different vertical rooting patterns determined by specific interactions between hydrologic properties and rooting. Lafleur et al. (2005) and Schwärzel et al. (2006) found much deeper WTD thresholds for reductions in vascular transpiration that negatively affected vascular GPP over a Canadian pristine bog and a German drained fen, respectively. Those WTD thresholds were ~ 0.65 and ~ 0.9 m below the surface for the pristine and drained peatland, respectively, further indicating the importance of root–hydrology interactions and the resultant root adaptations, growth and uptake in determining WTD effects on vascular GPP across peatlands.

5.2 Divergences between modeled and EC-derived annual GPP, R_e and NEP

Modeled seasonal and annual GPP and R_e were consistently larger than EC-derived estimates of GPP and R_e during 2004–2009 (Fig. 7b, c, f, g). Although modeled annual GPP and R_e were larger than the EC-derived estimates, modeled annual NEP was consistently lower than the EC gap-filled annual NEP (Fig. 7e). Modeled annual NEP was smaller than

EC gap-filled NEP since the divergence between modeled and EC-derived R_e was larger than the deviation between modeled and EC-derived GPP (Fig. 7f, g). Modeled R_e were larger than EC-derived R_e mainly due to the presence of gap-filled nighttime CO_2 fluxes (= R_e) in EC-derived R_e, which were smaller than corresponding modeled values. This was apparent in negative intercepts that resulted from regressions of modeled vs. gap-filled net CO_2 fluxes (Table S1 in the Supplement). Gap-filled R_e fluxes were calculated from soil temperature (T_s) at a shallow depth (0.05 m) (Sect. 3.2.2). During nighttime and in the winter, peat at this shallow depth rapidly cooled down, which produced smaller nighttime gap-filled CO_2 fluxes empirically derived from lower T_s (Figs. 3, 5 and 6). By contrast, corresponding modeled CO_2 effluxes were affected by not only the cooler shallow peat layers but also the warmer deeper peat layers and thus were larger than the gap-filled fluxes (e.g., Figs. 5a, 6h, i). Like modeled CO_2 effluxes, chamber-measured soil and understory CO_2 effluxes in cooler nights did not decline as rapidly as did the corresponding gap-filled net ecosystem CO_2 fluxes as night progressed, which further indicated the likely contribution of a gap-filling artifact to CO_2 effluxes that were smaller than corresponding modeled fluxes (e.g., Figs. 5b vs. a, 6j–k vs. g–h).

Systematic uncertainties embedded in EC methodology could also have contributed to EC-derived annual and growing season R_e which was smaller than the modeled values (Fig. 7c, g). The major uncertainty in the EC methodology is the possible underestimation of nighttime EC CO_2 flux measurements due to poor turbulent mixing under stable air conditions (Goulden et al., 1997; Miller et al., 2004). By contrast, modeled biological production of CO_2 by plant and microbial respiration was independent of turbulent mixing, which could thus contribute to modeled R_e that was larger than EC-derived estimates.

Complete energy balance closure in the model as opposed to incomplete (~ 75 %) energy balance closure in EC measurements would also give rise to modeled evapotranspiration and GPP values that were larger than EC-derived estimates (Fig. 7b, f) (Mezbahuddin et al., 2016). Modeled GPP influenced modeled R_e through root exudation and litter fall (Fig. 1). Therefore, modeled GPP that was larger than EC-derived estimates would have further contributed to modeled growing season and annual R_e that was larger than EC-derived estimates (Fig. 7c, g).

Modeled GPP and hence R_e larger than EC-derived estimates could also be a result of uncertainties in model inputs for soil organic N, N deposition, N_2 fixation and any other sources of N inputs into the modeled ecosystem. In ecosys, plant productivity is governed by foliar N status, which is constrained by root N availability and uptake. Our input for organic N into each modeled peat layer was measured for corresponding depth at the site (Fig. 2). To simulate N deposition, background wet deposition rates of 0.5 mg ammonium-N, and 0.25 mg nitrate-N per liter of precipi-

tation were used as model inputs. However, from visual field observations, it was evident that there was a significant amount of nutrient inflow with the lateral water influxes into this fen peatland from the surrounding upland forests; this inflow was not quantified. To mimic this lateral nutrient inflow, we doubled the background wet deposition of NH_4^+ and NO_3^- as reported for the area and used these as surrogates of lateral nutrient inflows into the modeled ecosystem. Ecosys also included an N_2 fixing algorithm which simulated symbiotic N_2 fixation in moss canopies that was reported for the boreal forests (Sect. 3.2.3). We tested the adequacy of these N inputs into the model by comparing modeled leaf N concentrations against those measured in the field. The modeled foliar N concentrations for all the vascular PFTs compared well to site measurements (Table 2). To further examine the contribution of uncertainty due to model inputs towards the divergence between modeled and EC-derived seasonal and annual GPP and R_e, we performed a sensitivity test where we had a parallel run without doubling the background N wet deposition rates in the model, hence simulating no lateral N influx into the modeled ecosystem. Unlike the run with lateral N inflow, the parallel run without lateral N inflow simulated GPP and R_e, which were very close to the EC-derived estimates. However, the regressions between hourly modeled net CO_2 fluxes from the parallel run and EC-measured hourly net CO_2 fluxes gave slopes of ~ 0.8, indicating under-simulation of the EC-measured fluxes in the parallel run with no lateral N inflow.

6 Conclusions

Our modeling study showed that, when adequately coupled to algorithms of a process-based ecosystem model, the existing knowledge of peatland eco-hydrological and biogeochemical processes could explain underlying mechanisms that governed WTD effects on net ecosystem CO_2 exchange of a boreal fen. Testing of our hypotheses against EC-measured net CO_2 fluxes, automated chamber fluxes and other biometric measurements at the site revealed that a drier-weather-driven WTD drawdown at this boreal fen raised both R_e and GPP due to improved aeration that facilitated (1) microbial and root O_2 availability, energy yields, growth and decomposition, which raised microbial and root respiration; and (2) rapid nitrogen mineralization and consequently increased root nitrogen availability and uptake that improved leaf nitrogen status and hence raised carboxylation (Figs. 1, 7, 8) (Table 2). Similar increases in R_e and GPP with WTD drawdown to a certain depth caused no net WTD drawdown effect on NEP (Fig. 8). Modeled drainage projection, however, showed that further WTD drawdown caused by either drainage or climate-change-induced drying would produce plant water stress and reduce GPP and hence NEP of this boreal fen (Figs. 9, 10). This study further reconciled and mechanistically explained the WTD effects on seasonal and

annual GPP, R_e and hence NEP of this boreal fen, on which there was previously speculation on the basis of EC-derived estimates. However, although modeled CO_2 fluxes were validated well by the EC and chamber-measured net CO_2 fluxes, modeled values of annual and seasonal GPP and R_e were consistently larger than the EC-derived estimates (Table 1) (Figs. 7, 8) (Sect. 5.2). These discrepancies between modeled and EC-derived GPP and R_e estimates also created an opportunity of value addition by using more robust process-based estimates while forecasting WTD effects on these peatland C balance components in addition to empirically modeled EC-derived estimates that might not include some of the above-discussed offsetting feedbacks in peatland eco-hydrology and biogeochemistry.

The model algorithms that were used in this study represented coupled feedbacks among ecosystem processes that governed carbon, water, energy and nutrient (N, P) cycling in a peatland ecosystem. These feedbacks were thus not parameterized for this particular boreal fen peatland site. Instead, the modeled boreal fen was simulated from peatland-specific model inputs for weather, soil and vegetation properties that had physical meaning and were quantifiable at the site (Fig. 2). These modeled process-level interactions were also validated by corroborating modeled outputs against site measurements. By contrast, most of the current peatland C models use scalar functions to represent these feedbacks, and so those model algorithms have to be parameterized for each peatland site. Therefore, the modeling approach as described in this study should be more robust than the scalar feedback approach while assessing WTD effects on peatland C balance under contrasting peat types, climates and hydrology or under unknown future climates. These process-level feedbacks are also scalable once the peatlands of interest are defined within the modeled landscapes by scalable model inputs for weather; peat hydrological, physical, and biological properties; and plant functional types (Sect. 3.3.3). Current global land surface models either lack or have very poor representation of these feedbacks, which is thus far limiting our large-scale predictive capacity of WTD effects on boreal peatland C stocks. This modeling exercise would thus provide valuable information to improve the representation of these feedbacks into next-generation land surface models. Therefore, the insights gained from this modeling study should be a significant contribution to our understanding and apprehension of how peatlands would behave with changing hydrology under future drier and warmer climates.

The Supplement related to this article is available online at https://doi.org/10.5194/bg-14-5507-2017-supplement.

Author contributions. MM contributed to the model code modification and development, the design of the modeling experiment, simulation, validation and analyses of modeled outputs. RFG is the original developer of the model ecosys and also contributed to simulation design and model runs. LBF was site principal investigator, who led the collection and quality control of the field data that were used to validate model outputs. MM wrote the manuscript with significant contributions from RFG and LBF.

References

Aerts, R. and Chapin III, F.: The mineral nutrition of wild plants revisited: a re-evaluation of processes and patterns, Adv. Ecol. Res., 30, 1–67, https://doi.org/10.1016/S0065-2504(08)60016-1, 1999.

Baker, I. T., Prihodko, L., Denning, A. S., Goulden, M., Miller, S., and Da Rocha, H. R.: Seasonal drought stress in the Amazon: reconciling models and observations, J. Geophys. Res.-Biogeo., 113, G00B01, https://doi.org/10.1029/2007JG000644, 2008.

Ballantyne, D. M., Hribljan, J. A., Pypker, T. G., and Chimner, R. A.: Long-term water table manipulations alter peatland gaseous carbon fluxes in Northern Michigan, Wetl. Ecol. Manag., 22, 35–47, https://doi.org/10.1007/s11273-013-9320-8, 2014.

Barr, A. G., Black, T. A., Hogg, E. H., Kljun, N., Morgenstern, K., and Nesic, Z.: Inter-annual variability in the leaf area index of a boreal aspen-hazelnut forest in relation to net ecosystem production, Agric. For. Meteorol. 126, 237–255, https://doi.org/10.1016/j.agrformet.2004.06.011, 2004.

Bond-Lamberty, B., Gower, S. T., and Ahl, D. E.: Improved simulation of poorly drained forests using Biome-BGC, Tree Physiol., 27, 703–715, https://doi.org/10.1093/treephys/27.5.703, 2007.

Cai, T., Flanagan, L. B., and Syed, K. H.: Warmer and drier conditions stimulate respiration more than photosynthesis in a boreal peatland ecosystem: analysis of automatic chambers and eddy covariance measurements, Plant Cell Environ., 33, 394–407, https://doi.org/10.1111/j.1365-3040.2009.02089.x, 2010.

Campbell, G. S.: A simple method for determining unsaturated conductivity from moisture retention data, Soil Sci., 117, 311–314, 1974.

Choi, W. J., Chang, S. X., and Bhatti, J. S.: Drainage affects tree growth and C and N dynamics in a minerotrophic peatland, Ecology, 88, 443–453, https://doi.org/10.1890/0012-9658(2007)88[443:DATGAC]2.0.CO;2, 2007.

Cronk, J. K. and Fennessy, M. S.: Wetland plants: biology and ecology, 1st edition, Boca Raton, CRC press, 482 pp. 2001.

Dimitrov, D. D., Grant, R. F., Lafleur, P. M., and Humphreys, E. R.: Modeling the effects of hydrology on ecosystem respiration at Mer Bleue bog, J. Geophys. Res.-Biogeo., 115, G04043, https://doi.org/10.1029/2010JG001312, 2010a.

Dimitrov, D. D., Grant, R. F., Lafleur, P. M., and Humphreys, E. R.: Modelling subsurface hydrology of Mer Bleue bog, Soil Sci. Soc. Am. J., 74, 680–694, https://doi.org/10.2136/sssaj2009.0148, 2010b.

Dimitrov, D. D., Grant, R. F., Lafleur, P. M., and Humphreys, E. R.: Modeling the effects of hydrology on gross primary productivity and net ecosystem productivity at Mer Bleue bog, J. Geophys. Res.-Biogeo., 116, G04010, https://doi.org/10.1029/2010JG001586, 2011.

Dise, N. B: Peatland response to global change, Science, 326, 810–811, https://doi.org/10.1126/science.1174268, 2009.

Flanagan, L. B. and Syed, K. H.: Stimulation of both photosynthesis and respiration in response to warmer and drier conditions in a boreal peatland ecosystem, Glob. Change Biol., 17, 2271–2287, https://doi.org/10.1111/j.1365-2486.2010.02378.x, 2011.

FLUXNET Canada Team: FLUXNET Canada Research Network – Canadian Carbon Program Data Collection, 1993–2014, ORNL DAAC, Oak Ridge, Tennessee, USA, https://doi.org/10.3334/ORNLDAAC/1335, 2016.

Frolking, S., Roulet, N. T., Moore, T. R., Lafleur, P. M., Bubier, J. L., and Crill, P. M.: Modelling the seasonal to annual carbon balance of Mer Bleue bog, Ontario, Canada, Global Biogeochem. Cy., 16, 1–21, https://doi.org/10.1029/2001GB001457, 2002.

Gerten, D., Schaphoff, S., Haberlandt, U., Lucht, W., and Sitch, S.: Terrestrial vegetation and water balance-hydrological evaluation of a dynamic global vegetation model, J. Hydrol., 286, 249–270, https://doi.org/10.1016/j.jhydrol.2003.09.029, 2004.

Gorham, E.: Northern peatlands: role in the carbon cycle and probable responses to climatic warming, Ecol. Appl., 1, 182–195, https://doi.org/10.2307/1941811, 1991.

Goulden, M. L., Daube, B. C., Fan, S. M., Sutton, D. J., Bazzaz, A., Munger, J. W., and Wofsy, S. C.: Physiological responses of a black spruce forest to weather, J. Geophys. Res.-Atmos., 102, 28987–28996, https://doi.org/10.1029/97JD01111, 1997.

Grant, R. F., Desai, A. R., and Sulman, B. N.: Modelling contrasting responses of wetland productivity to changes in water table depth, Biogeosciences, 9, 4215–4231, https://doi.org/10.5194/bg-9-4215-2012, 2012.

Ise, T., Dunn, A. L., Wofsy, S. C., and Moorcroft, P. R.: High sensitivity of peat decomposition to climate change through water-table feedback, Nat. Geosci., 1, 763–766, https://doi.org/10.1038/ngeo331, 2008.

Kotowska, A: The long-term effects of drainage on carbon cycling in a boreal fen, M. Sc. thesis, Department of Integrative Biology, University of Guelph, Ontario, Canada, 75 pp., 2013.

Krinner, G., Viovy, N., de Noblet-Ducoudré, N., Ogée, J., Polcher, J., Friedlingstein, P., Ciais, P., Sitch, S., and Prentice, I. C.: A dynamic global vegetation model for studies of the coupled atmosphere-biosphere system, Global Biogeochem. Cy., 19, GB1015, https://doi.org/10.1029/2003GB002199, 2005.

Kuiper, J. J., Mooij, W. M., Bragazza, L., and Robroek, B. J.: Plant functional types define magnitude of drought response in peatland CO_2 exchange, Ecology, 95, 123–131, https://doi.org/10.1890/13-0270.1, 2014.

Lafleur, P. M., Hember, R. A., Admiral, S. W., and Roulet, N. T.: Annual and seasonal variability in evapotranspiration and water table at a shrub-covered bog in southern Ontario, Canada, Hydrol. Process., 19, 3533–3550, https://doi.org/10.1002/hyp.5842, 2005.

Lieffers, V. J. and Rothwell, R. L.: Rooting of peatland black spruce and tamarack in relation to depth of water table, Can. J. Botany, 65, 817–821, https://doi.org/10.1139/b87-111, 1987.

Limpens, J., Berendse, F., Blodau, C., Canadell, J. G., Freeman, C., Holden, J., Roulet, N., Rydin, H., and Schaepman-Strub, G.: Peatlands and the carbon cycle: from local processes to global implications – a synthesis, Biogeosciences, 5, 1475–1491, https://doi.org/10.5194/bg-5-1475-2008, 2008.

Lizama, H. M. and Suzuki, I.: Kinetics of sulfur and pyrite oxidation by Thiobacillus thiooxidans. Competitive inhibition by increasing concentrations of cells, Can. J. Microbiol., 37, 182–187, https://doi.org/10.1139/m91-028, 1991.

Long, K. D., Flanagan, L. B., and Cai, T.: Diurnal and seasonal variation in methane emissions in a northern Canadian peatland measured by eddy covariance, Glob. Change Biol. 16, 2420–2435, https://doi.org/10.1111/j.1365-2486.2009.02083.x, 2010.

Long, K. D.: Methane fluxes from a northern peatland: mechanisms controlling diurnal and seasonal variation and the magnitude of aerobic methanogenesis, M.Sc. thesis, Department of Biological Sciences, University of Lethbridge, Lethbridge, AB, Canada, 100 pp., 2008.

Macdonald, S. E. and Lieffers, V. J.: Photosynthesis, water relations, and foliar nitrogen of Picea mariana and Larix laricina from drained and undrained peatlands, Can. J. Forest Res., 20, 995–1000, https://doi.org/10.1139/x90-133, 1990.

Mäkiranta, P., Laiho, R., Fritze, H., Hytönen, J., Laine, J., and Minkkinen, K.: Indirect regulation of heterotrophic peat soil respiration by water level via microbial community structure and temperature sensitivity, Soil Biol. Biochem., 41, 695–703, https://doi.org/10.1016/j.soilbio.2009.01.004, 2009.

Markham, J. H.: Variation in moss-associated nitrogen fixation in boreal forest stands, Oecologia 161, 353–359, https://doi.org/10.1007/s00442-009-1391-0, 2009.

Mettrop, I. S., Cusell, C., Kooijman, A. M., and Lamers, L. P.: Nutrient and carbon dynamics in peat from rich fens and Sphagnum-fens during different gradations of drought, Soil Biol. Biochem., 68, 317–328, https://doi.org/10.1016/j.soilbio.2013.10.023, 2014.

Mezbahuddin, M., Grant, R. F., and Hirano, T.: How hydrology determines seasonal and interannual variations in water table depth,

surface energy exchange, and water stress in a tropical peatland: modeling versus measurements, J. Geophys. Res.-Biogeo., 120, 2132–2157, https://doi.org/10.1002/2015JG003005, 2015.

Mezbahuddin, M., Grant, R. F., and Hirano, T.: Modelling effects of seasonal variation in water table depth on net ecosystem CO_2 exchange of a tropical peatland, Biogeosciences, 11, 577–599, https://doi.org/10.5194/bg-11-577-2014, 2014.

Mezbahuddin, M., Grant, R. F., and Flanagan, L. B.: Modeling hydrological controls on variations in peat water content, water table depth, and surface energy exchange of a boreal western Canadian fen peatland, J. Geophys. Res.-Biogeo., 121, 2216–2242, https://doi.org/10.1002/2016JG003501, 2016.

Miller, S. D., Goulden, M. L., Menton, M. C., da Rocha, H. R., de Freitas, H. C., Figueira, A. M. e. S., and de Sousa, C. A. D.: Biometric and micrometeorological measurements of tropical forest carbon balance, Ecol. Appl., 14, 114–126, https://doi.org/10.1890/02-6005, 2004.

Moore, T. and Basiliko, N.: Decomposition in boreal peatlands, in: Boreal peatland ecosystems, edited by: Wieder, R. K. and Vitt, D. H., Springer Science & Business Media, 125–143, 2006.

Munir, T. M., Xu, B., Perkins, M., and Strack, M.: Responses of carbon dioxide flux and plant biomass to water table drawdown in a treed peatland in northern Alberta: a climate change perspective, Biogeosciences, 11, 807–820, https://doi.org/10.5194/bg-11-807-2014, 2014.

Murphy, M., Laiho, R., and Moore, T. R.: Effects of water table drawdown on root production and aboveground biomass in a boreal bog, Ecosystems, 12, 1268–1282, https://doi.org/10.1007/s10021-009-9283-z, 2009.

Parmentier, F. J. W., Van der Molen, M. K., de Jeu, R. A. M., Hendriks, D. M. D., and Dolman, A. J.: CO_2 fluxes and evaporation on a peatland in the Netherlands appear not affected by water table fluctuations, Agr. Forest Meteorol., 149, 1201–1208, https://doi.org/10.1016/j.agrformet.2008.11.007, 2009.

Peichl, M., Öquist, M., Löfvenius, M. O., Ilstedt, U., Sagerfors, J., Grelle, A., Lindroth, A., and Nilsson, M. B.: A 12-year record reveals pre-growing season temperature and water table level threshold effects on the net carbon dioxide exchange in a boreal fen, Environ. Res. Lett., 9, 055006, https://doi.org/10.1088/1748-9326/9/5/055006, 2014.

Preston, M. D., Smemo, K. A., McLaughlin, J. W., and Basiliko, N.: Peatland microbial communities and decomposition processes in the James Bay Lowlands, Canada, Front. Microbiol., 3, 70, https://doi.org/10.3389/fmicb.2012.00070, 2012.

Richardson, A. D., Hollinger, D. Y., Burba, G. G., Davis, K. J., Flanagan, L. B., Katul, G. G., Munger, J. W., Ricciuto, D. M., Stoy, P. C., Suyker, A. E., Verma, S. B., and Wofsy, S. C.: A multi-site analysis of random error in tower-based measurements of carbon and energy fluxes, Agr. Forest Meteorol., 136, 1–18, https://doi.org/10.1016/j.agrformet.2006.01.007, 2006.

Rippy, J. F. and Nelson, P. V.: Cation exchange capacity and base saturation variation among Alberta, Canada, moss peats, HortScience, 42, 349–352, 2007.

Riutta, T., Laine, J., and Tuittila, E. S.: Sensitivity of CO_2 exchange of fen ecosystem components to water level variation, Ecosystems, 10, 718–733, https://doi.org/10.1007/s10021-007-9046-7, 2007.

Riutta, T.: Fen ecosystem carbon gas dynamics in changing hydrological conditions, Diss. For. 67, Department of Forest Ecol-

ogy, Faculty of Agriculture and Forestry, University of Helsinki, 46 pp., 2008.

Schaefer, K., Collatz, G. J., Tans, P., Denning, A. S., Baker, I., Berry, J., Prihodko, L., Suits, N., and Philpott, A.: Combined simple biosphere/Carnegie-Ames-Stanford approach terrestrial carbon cycle model, J. Geophys. Res.-Biogeo., 113, G03034, https://doi.org/10.1029/2007JG000603, 2008.

Schwärzel, K., Šim°unek, J., van Genuchten, M. T., and Wessolek, G.: Measurement and modeling of soil-water dynamics and evapotranspiration of drained peatland soils, J. Plant Nutr. Soil Sci., 169, 762–774, https://doi.org/10.1002/jpln.200621992, 2006.

Sonnentag, O., van der Kamp, G., Barr, A. G., and Chen, J. M.: On the relationship between water table depth and water vapour and carbon dioxide fluxes in a minerotrophic fen, Glob. Change Biol., 16, 1762–1776, https://doi.org/10.1111/j.1365-2486.2009.02032.x, 2010.

St-Hilaire, F., Wu, J., Roulet, N. T., Frolking, S., Lafleur, P. M., Humphreys, E. R., and Arora, V.: McGill wetland model: evaluation of a peatland carbon simulator developed for global assessments, Biogeosciences, 7, 3517–3530, https://doi.org/10.5194/bg-7-3517-2010, 2010.

Strack, M., Waddington, J. M., Rochefort, L., and Tuittila, E. S.: Response of vegetation and net ecosystem carbon dioxide exchange at different peatland microforms following water table drawdown, J. Geophys. Res.-Biogeo., 111, G02006, https://doi.org/10.1029/2005JG000145, 2006.

Sulman, B. N., Desai, A. R., Cook, B. D., Saliendra, N., and Mackay, D. S.: Contrasting carbon dioxide fluxes between a drying shrub wetland in Northern Wisconsin, USA, and nearby forests, Biogeosciences, 6, 1115–1126, https://doi.org/10.5194/bg-6-1115-2009, 2009.

Sulman, B. N., Desai, A. R., Saliendra, N. Z., Lafleur, P. M., Flanagan, L. B., Sonnentag, O., Mackay, D. S., Barr, A. G., and van der Kamp, G.: CO_2 fluxes at northern fens and bogs have opposite responses to inter-annual fluctuations in water table, Geophys. Res. Lett., 37, L19702, https://doi.org/10.1029/2010GL044018, 2010.

Sulman, B. N., Desai, A. R., Schroeder, N. M., Ricciuto, D., Barr, A., Richardson, A. D., Flanagan, L. B., Lafleur, P. M., Tian, H., Chen, G., Grant, R. F., Poulter, B., Verbeeck, H., Ciais, P., Ringeval, B., Baker, I. T., Schaefer, K., Luo, Y., and Weng, E.: Impact of hydrological variations on modeling of peatland CO_2 fluxes: Results from the North American Carbon Program site synthesis, J. Geophys. Res.-Biogeo., 117, G01031, https://doi.org/10.1029/2011JG001862, 2012.

Syed, K. H., Flanagan, L. B., Carlson, P. J., Glenn, A. J., and Van Gaalen, K. E.: Environmental control of net ecosystem CO_2 exchange in a treed, moderately rich fen in northern Alberta, Agr. Forest Meteorol., 140, 9–114, https://doi.org/10.1016/j.agrformet.2006.03.022, 2006.

Tian, H., Chen, G., Liu, M., Zhang, C., Sun, G., Lu, C., Xu, X., Ren, W., Pan, S., and Chappelka, A.: Model estimates of net primary productivity, evapotranspiration, and water use efficiency in the terrestrial ecosystems of the southern United States during 1895–2007, Forest Ecol. Manag., 259, 1311–1327, https://doi.org/10.1016/j.foreco.2009.10.009, 2010.

Turunen, J., Tomppo, E., Tolonen, K., and Reinikainen, A.: Estimating carbon accumulation rates of undrained mires in Finland-

application to boreal and subarctic regions, The Holocene, 12, 69–80, 2002.

Updegraff, K., Pastor, J., Bridgham, S. D., and Johnston, C. A.: Environmental and substrate controls over carbon and nitrogen mineralization in northern wetlands, Ecol. Appl., 5, 151–163, https://doi.org/10.2307/1942060, 1995.

van Genuchten, M. T.: A closed-form equation for predicting the hydraulic conductivity of unsaturated soils, Soil Sci. Soc. Amer. J., 44, 892–898, https://doi.org/10.2136/sssaj1980.03615995004400050002x, 1980.

Waddington, J. M., Morris, P. J., Kettridge, N., Granath, G., Thompson, D. K., and Moore, P. A.: Hydrological feedbacks in northern peatlands, Ecohydrology, 8, 113–127, https://doi.org/10.1002/eco.1493, 2015.

Weng, E. and Luo, Y.: Soil hydrological properties regulate grassland ecosystem responses to multifactor global change: A modeling analysis, J. Geophys. Res.-Biogeo., 113, G03003, https://doi.org/10.1029/2007JG000539, 2008.

Wesely, M. L. and Hart, R. L.: Variability of short term eddy-correlation estimates of mass exchange, in: The ForestAtmosphere Interaction, edited by: Hutchinson, B. A., Hicks, B. B., and Reidel, D., 591–612, Dordrecht, 1985.

Wu, J., Kutzbach, L., Jager, D., Wille, C., and Wilmking, M.: Evapotranspiration dynamics in a boreal peatland and its impact on the water and energy balance, J. Geophys. Res.-Biogeo., 115, G04038, https://doi.org/10.1029/2009JG001075, 2010.

Zhang, Y., Li, C., Trettin, C. C., Li, H., and Sun, G.: An integrated model of soil, hydrology, and vegetation for carbon dynamics in wetland ecosystems, Global Biogeochem. Cy., 16, 9-1-9-17, https://doi.org/10.1029/2001GB001838, 2002.